CONVEYOR BELT SPLICING IMPROVEMENT TECHNOLOGY

Sergio Alexander Cabrera
BE Mech, Monash University, Melbourne

A thesis submitted in fulfilment of the requirements for the degree of Master of Philosophy in Mechanical Engineering

This research was supported by an Australian Government Research Training Program (RTP) Scholarship

October 2019

University of Newcastle – School of Engineering

THE UNIVERSITY OF NEWCASTLE AUSTRALIA

STATEMENT OF ORIGINALITY

I hereby certify that the work embodied in the thesis is my own work, conducted under normal supervision. The thesis contains no material which has been accepted, or is being examined, for the award of any other degree or diploma in any university or other tertiary institution and, to the best of my knowledge and belief, contains no material previously published or written by another person, except where due reference has been made. I give consent to the final version of my thesis being made available worldwide when deposited in the University's Digital Repository, subject to the provisions of the Copyright Act 1968 and any approved embargo.

Sergio Cabrera

ACKNOWLEDGMENT

I would first like to thank my thesis supervisor Professor Wheeler of the School of Engineering at Newcastle University. Even though I was an off-campus student, I was still able to get help whenever I ran into a trouble spot or had a question about my research or writing. His direction and guidance have been invaluable to my work.

I would also like to thank Mitch Gibbs for his technical assistance with testing of all belt splice assemblies with some done in my absence.

I would also like to acknowledge Professor Gary James and Associate Professor Chris Wensrich at the School of Engineering at the University of Newcastle as the additional readers of this thesis, and I am gratefully indebted to their valuable comments on this thesis.

Finally, I must express my very profound gratitude to my friends, parents and especially to my wife Kieta for providing me with support and continuous encouragement and late-night tea brews deliveries throughout my years of study and through and writing this thesis. This accomplishment would not have been possible without her. Thank you.

Sergio Cabrera

TABLE OF CONTENTS

FIGURES

TABLES

ABSTRACT

This work reviews current industry technology used for splicing steel cord and fabric conveyor belts. The focus is on the use of the ‘step method’, which splices belt ends together by vulcanising natural rubber, creating a bond between steel cords and fabric members. Investigation into the use of vulcanised rubber as a bonding medium raises concerns regarding its ability to sustain high loads under shear. Additional limitations arising from reliability, environmental affects and fatiguing were also highlighted as issues. Because of the shortfalls in current joining methods for steel cord belts, development of a new splicing technology has been proposed, with direct cord-to-cord joins with an adhesive bonded splice assembly. Preliminary Finite Element Analysis (FEA) indicates that a combination of cyanoacrylate/acrylic adhesives and a mechanically locking splice assembly can support high-tensile loads transferred through steel conveyor belt steel cords.

1 INTRODUCTION

The use of conveyors in industry over the last two centuries has helped reduce the cost of transporting bulk solids through plants, mines and ports worldwide. However, competitive markets and reduced margins have driven companies to increase production using existing infrastructure. Because of this, conveyor belts are being pushed past the maximum operating belt tensions; in some cases, potentially exceeding them. In addition to greater conveyor throughputs, cost savings have been found by reducing both scheduled and unscheduled downtime; conveyors are now operated with throughputs of 10,000 tonnes per hour or more for longer periods of time. With prices over 100USD per tonne as per May 2019[1], cost of conveyor downtime can exceed USD500,000 per hour.

Improvements in belt design, including lateral reinforcement for improved impact resistance, adhesive cover repairs and energy-saving rubber compounds that reduce power consumption when traveling over conveyor carry idlers, have improved the overall operational life of belts. Development and research into conveyor belt splicing technology has also moved forward, with belt suppliers providing better tools and simplifying the splicing process.

In addition to fabrication improvements, methods have been developed to protect belt splices via online monitoring using magnetic field signatures, which can detect steel cord elongation [2]. Even with these improvements, the process of joining steel cord belts using the step splicing method has fundamentally stayed the same; that is, laying cords adjacent to each other, creating a sandwich, using heat and pressure to vulcanise the splice. With ever-increasing demands on conveyor belts, quality and speed of splicing must improve. Current methods of splicing can take 12 hours or more to complete; this is to allow for preparation, manual labour and the unavoidable time required to vulcanise the rubber sandwich.

Increasing the speed and quality of belt splicing may potentially require an automated method to complete repetitive tasks such as skiving (stripping the belt back) and preparation for splicing. Eventually, this could lead to automation technology that might require only one person for the initial set up of equipment. Alternatively, the development of a small and simple joint method could be produced, with a potential concept utilising a type of structural adhesive. This would eliminate the need to use the vulcanisation process as a splice bond. By improving the joining method, more confidence could be gained, allowing engineers and asset owners to potentially select belts with lower strength ratings while still achieving minimum operating tensions.

Manufacture of conveyor belts is conducted in a controlled environment, ensuring that relevant standards are adhered to. Splicing done in exposed environments introduces construction errors, including incorrect cord spacing, bad preparation and environmental effects such as dust and high humidity. These have accumulative effects on a splice joint. Reducing construction time for each splice on site is accumulative, and any savings would translate to significant financial gains.

Fundamentally, as conveyor belt tensions increase, the ability to transition to pulleys and travel through curves and turnovers becomes increasingly important. As a conveyor belt travels through these geometries, the belt redistributes tension through the steel cord rubber matrix—how this is done through a conveyor belt splice is difficult to determine since rubber does not have a linear stress vs strain property and should be determined through testing. Finally, simplifying the whole splice fabrication process by proposing a new splicing concept along with removing the need to use vulcanisation to produce a bond will help overall with the quality and strength of the join. Moreover, by using linear engineering materials as opposed to rubber, it will be possible to better predict loads with greater confidence.

1.1 Research Objective

The objective of this research is to review current belt splicing technologies and determine the limitations that affect overall constructability and strength. The outcome of this research will assist with the development of an alternative splicing method and potentially improve existing ones.

1.2 Limitations and Assumptions

Best efforts have been made to construct splice assemblies accurately and in a consistent manner; however, since each assembly has been constructed manually (i.e., by hand, with hand tool in a non-controlled environment), minor inconsistencies may be present.

1.2.1 Component manufacturing

Because of the complex design of the splice assembly design concept, test components were 3D printed in a stainless steel (EOS Stainless Steel GP1) alloy. Printed components are comparable in strength to forged or cast metal components; depending on economies of scale, future mass production of parts may occur via 3D printing.

1.2.2 Assembly

Each splice assembly has been joined using a standard, readily available cyanoacrylate adhesive. Loctite brand was selected as this is a common, commercially available brand. A hybrid cyanoacrylate/epoxy resin has been proposed as the ideal bonding adhesive for use in mass production of splice assemblies; however, with its rapid set time of less than five seconds, it was not practical to use this type of hybrid adhesive during the development stage.

Because of time and limited access to environmentally controlled test facilities, cure time, humidity and temperature variations have not been considered variables affecting adhesive bond strength. Full bond strength has been assumed, as minimum curing times recommended by manufacturers were exceeded prior to commencement of testing splice assemblies.

1.2.3 FEA model

FEA models have been assembled in Strand 7 version 2.4.6., using a 64-bit operating system with Intel i7-6650U CPU @ 2.2GHz and 16GB RAM. Because of the large number of brick and beam elements required and limited computer processing capacity, the FEA models had to be simplified while minimising impact on accuracy. The geometric complexity of the steel wire rope has been simplified by combining all strands and wires used to make up its structure, creating a solid brick element cross section (see Figure 1.1).

Figure 1.1 Steel wire rope; (a) 7 x 7 pattern steel wire rope, (b) simplified finite element model for conveyor belt steel wire rope

Characteristics of steel wire rope and solid wire vary (e.g., flexibility and tensile strength); however, only the contact surface between the steel wire rope and ferrule is of importance here. This difference can be considered negligible when visually comparing images (a) and (b) (see Figure 1.2).

Ferrules connecting wires will also be made of steel wire rope. The diameter of the steel wire rope used will typically range between 1–1.5 mm in diameter and is tightly packed together. It can be assumed to be a solid circular cross section, as shown in Figure 1.2, to further reduce the complexity of finding a solution.

Figure 1.2 Steel wire rope; (a) 7 x 7 pattern steel wire rope, (b) simplified finite element model for ferrule steel wire rope connector

2 BACKGROUND

2.1 Conveyor Belt

Steel cord conveyor belts (Figure 2.1) are comprised of four main components, with cord type and quantity determining structural strength.

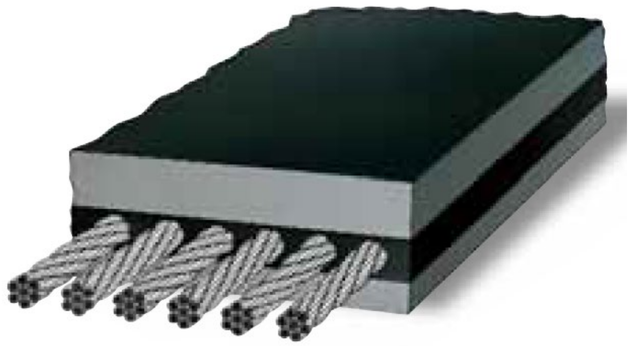

Figure 2.1 Steel cord belt with cover (top), steel cords and rubber gum (centre) and cover (bottom) [3]

Fabric reinforced conveyor belts (Figure 2.2) are comprised of three main components, with the number of plies used to determine belt strength.

Figure 2.2 Fabric belt with cover (top), fabric ply structural member (centre) and cover (bottom) [3]

Belt selection is based on both application requirements and belt tension within the conveyor system. Figure 2.3 summarises rated braking strength ranges for both.

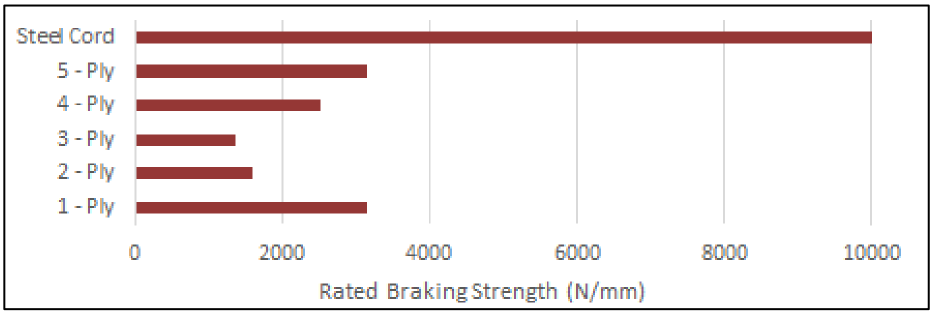

Figure 2.3 Steel cord and fabric belt rated braking summary in N/mm [4]

2.2 Splicing

A splice is required when joining two ends of a belt together on a conveyor installation, with large overland conveyor systems utilising multiple splice joints. Alternative methods of splicing methods (e.g., cold bonding (fabric belt only) and mechanical fastener splices) do exist, however for heavy industry, the step method is generally used.

2.2.1 Steel cord belt splicing

Steel cord belts are spliced together by placing exposed cord ends side by side in a geometric pattern called ‘steps’, as illustrated in Figure 2.4 below.

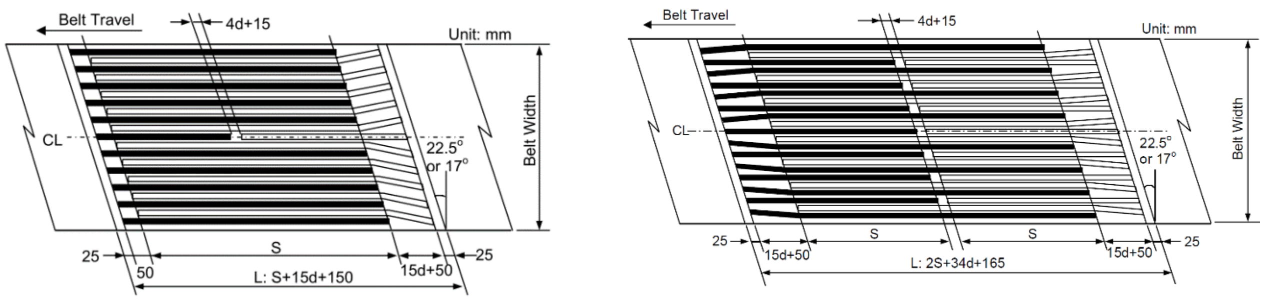

(a) (b)

Figure 2.4 Bridgestone steel cord splices; (a) one-step splice; (b) two-step splice, where L is splice length and S is step length [5]]

The number of steps is determined by the cord diameter (d) and the pitch (P) for each conveyor belt (Table 2.1).

Table 2.1 Bridgestone step selection criteria [5]

1 Step Method	$P \geq 2d + 3$ or $P \geq 5/2d$
2 Step Method	$P \geq 3/2d + 2.25$ or $P \geq 15/8d$
3 Step Method	$P \geq 2 + 3$ or $P > 7/5d$

Rubber gum strips are placed between cords, as shown in Figure 2.5, which will be vulcanised to bond cords together.

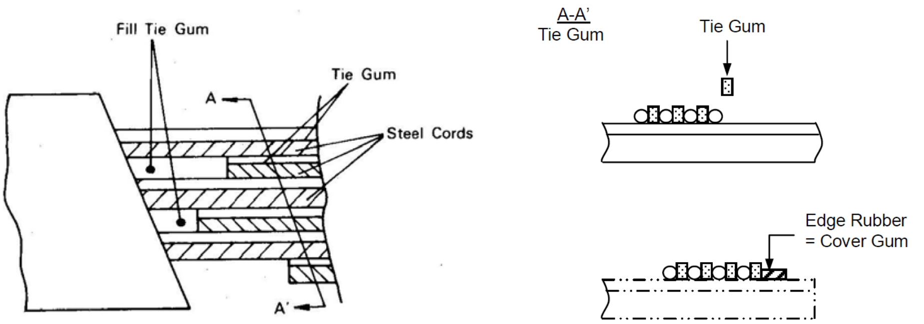

Figure 2.5 Bridgestone tie in gum method between steel cords [5]]

Splice covers are placed top and bottom before the sandwich of rubber and steel cords are placed under heat and pressure using a splice table (see Figure 2.6).

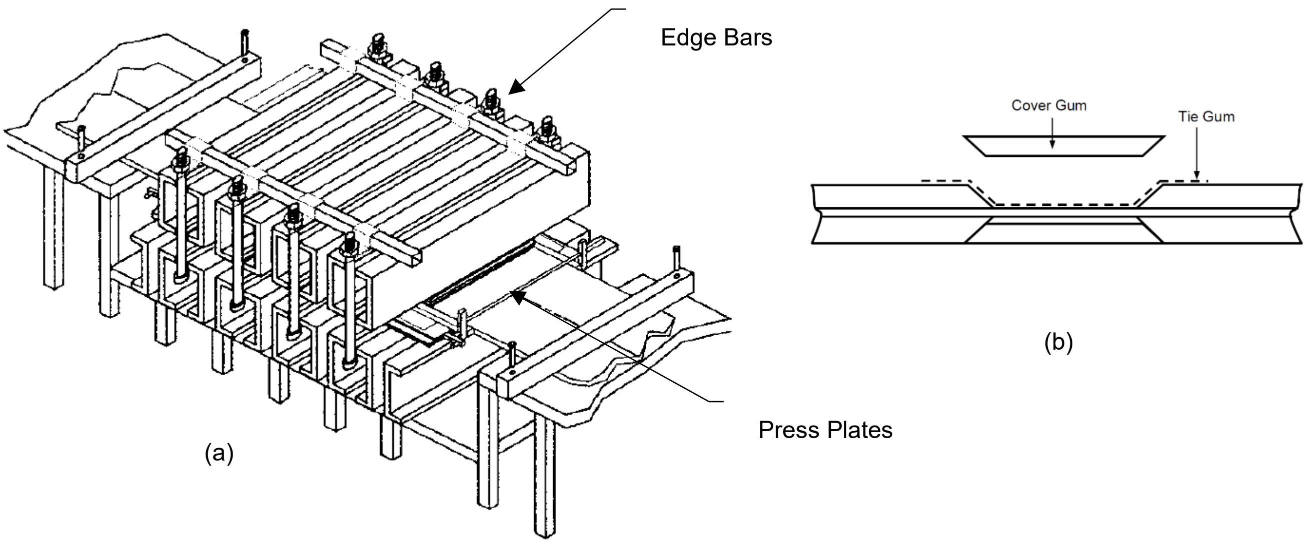

Figure 2.6 Splice assembly and vulcanisation; (a) vulcanising table with press plates and edge bars; (b) splice cover assembly [5]

The splice assembly is then clamped together with metal plates and edge bars to transfer even temperature and pressure.

2.2.2 Fabric belt splicing

Fabric belt can be spliced using equivalent step method as shown in Figure 2.7 below.

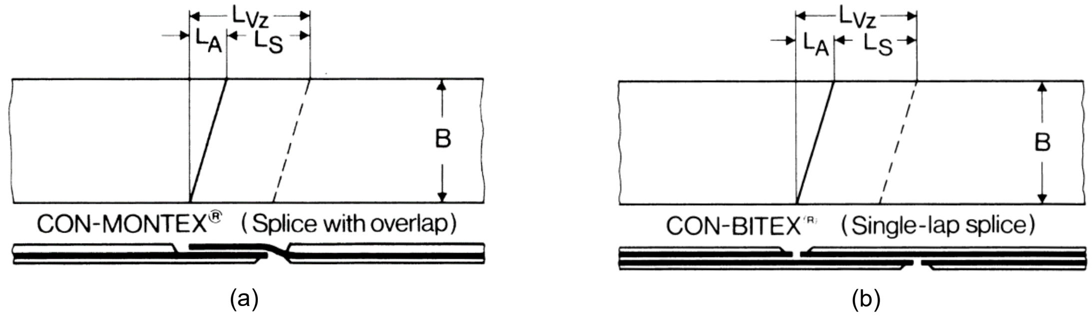

Figure 2.7 Fabric belt splice step; (a) Contitech overlap method; (b) Contitech single lap method where L_{Vz} is the splice length, L_s is the step length, L_A is the bias and B is belt width [6]

The overlap method is used when the belt only has one structural member; where two or more fabric members exist, each fabric member is layered in a staggered pattern, as shown above. Unvulcanised rubber sheets are placed between each structural member, and top and bottom covers are placed and then vulcanised to create the bond.

3 LITERATURE REVIEW

3.1 Introduction

Conveyor belt splice failures have been an ongoing issue within the mining industry since the introduction of conveyors over a century ago. To reduce failures, belt manufacturers are constantly developing technologies and monitoring methods to ensure splices are fabricated to the required standards. Unfortunately, belt splice failures still occur, resulting in a financial loss through unscheduled maintenance work and potentially causing injury or loss of human life. Because of time pressures, environmental conditions or lack of expertise, belt splicing using the step method is sometimes poorly fabricated, thereby not achieving the design rating. This shortens the lifespan of the splice, causing it to fail under lower operating belt tensions. Ongoing development will continue to improve the step method; however, while the design remains fundamentally unchanged, belt splice failures continue to occur.

The aim of this research is to inquire as to why rubber, a viscoelastic material with non-linear properties, is used to bond together linear property materials. Better understanding this process will lead to potentially more effective splicing alternatives.

3.2 Step Splice Construction

Because of the remote locations of most mines, such as that shown in Figure 3.1, belt splices are not always fabricated in ideal conditions.

Figure 3.1 Overland conveyor belt steel cord splice [7]

Dust, humidity and temperature extremes can affect the strength and reliability of a belt splice. Even small amounts of sweat trapped in the splice can boil, causing minor delamination during the vulcanising process. The German conveyor belt design standard DIN22101 attempts to take both workmanship and environmental conditions into account when fabricating the splice [4], by reducing the rating of the belt via a safety factor, S_0, shown in Table 3.1. An additional safety factor or dynamic efficiency characteristic, S_1, shown in Table 3.2, accounts for operating conditions and potential damage to the belt.

Table 3.1 Safety factor S_o based on manufacturer conditions of the splice [4]

Condition	Description of condition		
Atmosphere	normal	dust free	dusty
Protection from sunlight	normal	very good	poor
Ambient temperature	normal	≥ 18°C and ≤ 22°C	< 10°C or > 30°C
Working conditions	normal	spacious	narrow
Qualification of splicers	normal	very good	poor
Quality of splicing material	normal	fresh	close to expiration date
Quality of splicing press	normal	very good	poor
Safety factor S_0	1.1	causes	
		decrease	increase
		of the safety factor to	
		≥ 1.0	≤ 1.2

Table 3.2 Safety factor S_1 based on operating conditions [4]

Condition	Description of condition		
Life time	normal	low	high
Consequences of failure	normal	small	severe
Chemical/mechanical influence	normal	small	severe
Startups and stops	> 3 and < 30 per day	≤ 3 per day	≥ 30 per day
Revolution frequency	> 2 per hour and < 1 per minute	≤ 2 per hour	≥ 1 per minute
Safety factor S_1	1.7	causes	
		decrease	increase
		of the safety factor to	
		≥ 1.5	≤ 1.9

To prevent belt splice damage due to excessive tensions and environment, the minimum belt rating k_{tmin} required is:

$$\mathrm{k_N \geq k_{tmin} = \frac{c_k . S_0 . S_1 . k_{kmax}}{k_{trel}}} \qquad 1$$

where k_N is the rated belt strength, k_{trel} relative reference time strength (belt property), c_k a belt constant and k_{kmax} the maximum temporarily occurring tension at the belt edge. Equation 1 shows that as the product of $S_0.S_1$ increases, so does the minimum belt rating required to maintain a sufficient belt safety factor, and that improvement and simplification of the splicing process will act to reduce splice failure.

A paper presented by Otrebski and Saunders [8] also assesses the difficulties of splicing steel cord belts specifically, and suggests that the main factors affecting belt splices arise from the discontinuity of the conveyor belt cords; that is, no cord-to-cord contact, cord distribution and deformation within the splice itself. Otrebski and Saunders explain that shear stress is not uniform across cords since when steel cords are circular (see Figure 3.2), stress will be highest at the centre and lowest at the top and bottom between cords.

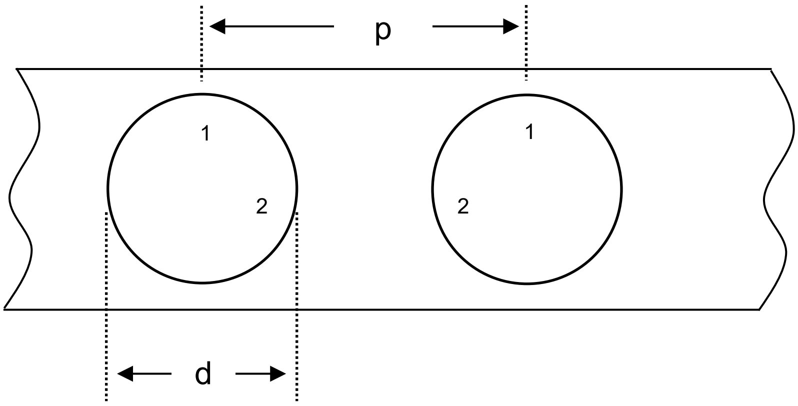

Figure 3.2 Simplified belt section steel cord pitch, p, and diameter, d with higher stress at point 2

Belt manufacturers limit this effect by optimising the pitch and cord diameter ratio (p/d) based on in-house development and this can therefore vary between conveyor belt suppliers. In practice, however, a ratio of 0.25–0.5 has been observed [8]. Fundamentally, Otrebski and Saunders' paper shows that symmetry and uniformity of the splice is one of the most important aspects and belt splice design. Variation in cord spacings will cause irregular stress distributions across the splice, thereby weakening it. Modelling by Song, Shang and Li on steel cord conveyor belt splices emphasises the importance of even cord distribution in a splice [9]. Finite element modelling was conducted, with the illustrated results shown in Figure 3.3 below.

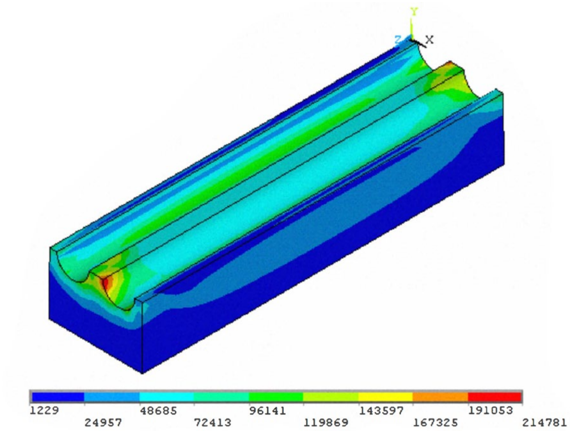

Figure 3.3 FEA results from steel cord splice under tension [9]

It is evident that the highest stress is found at the closest point between cords. This reinforces the importance of even cord distribution.

To ensure accurate cord spacings, Goodyear manufactures splice kits with pre-form panels (see Figure 3.4) [10]. The panel provides the pre-set spacing and prevents lateral movement of the cords during the vulcanising process.

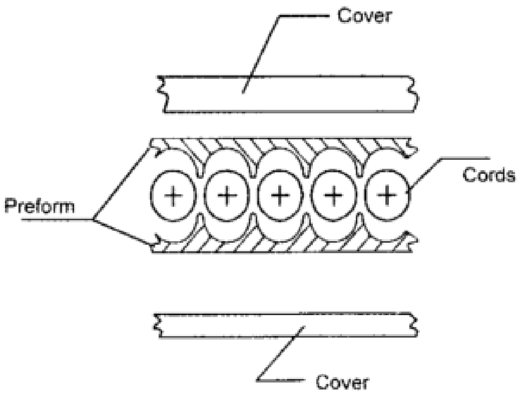

Figure 3.4 Goodyear pre-form panels [10]

This method ensures that spacing is even and because there are fewer components (e.g., rubber sheets and tie in gum), there is a saving in time and improvement in fabrication quality. Further, the simplicity lends itself to automation, which can further improve splice build.

A paper by Alexander Harrison on the limitations of theoretical splice design goes further, by discussing the less obvious causes of belt splice failure [11]. Harrison points out that impact from rock or ice can cause broken cord ruptures. Additional factors that can weaken a splice include excessive sag at chute loading points and even rapid cycling enough to cause resonance with the conveyor itself.

Like Otrebski and Saunders, Harrison investigates how cords are arranged, both in the horizontal plane and vertical misalignment (see Figure 3.5), which can occur during the vulcanisation process.

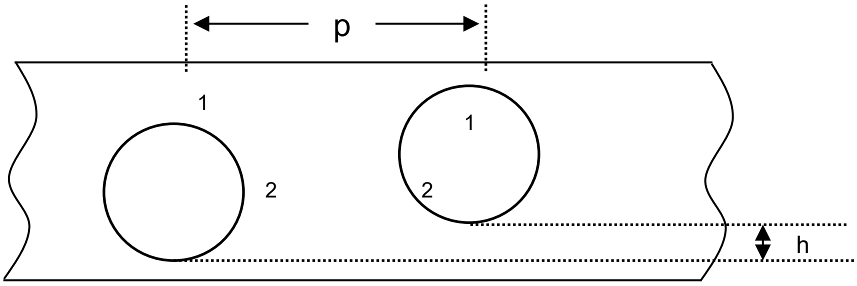

Figure 3.5 Vertical misalignment of cords in a steel cord splice, h

Again, this cord migration will cause further irregular stresses within the splice, further weakening the belt splice. The above discussion highlights the limitations of the step method, as weaknesses can be introduced at points during the splicing process. Some causes are not always noticeable, and using imaging equipment may not always be practical, cost effective or even capable of picking up defects with the required level of accuracy.

3.3 Rubber Strength

It is important that the rubber between conveyor belt steel cords bonds correctly during vulcanisation. Once a splice is under tension, the load is transferred to the vulcanised rubber strips, bonding the cords and fabric members together (see Figure 3.6)

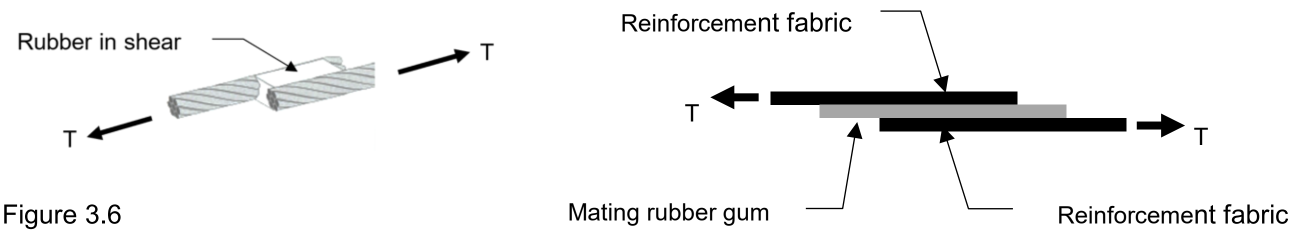

Figure 3.6 (a) Steel cords and (b) under tension, T, creating shear in bonding rubber gum

Figure 3.7 illustrates how shear in the rubber is produced.

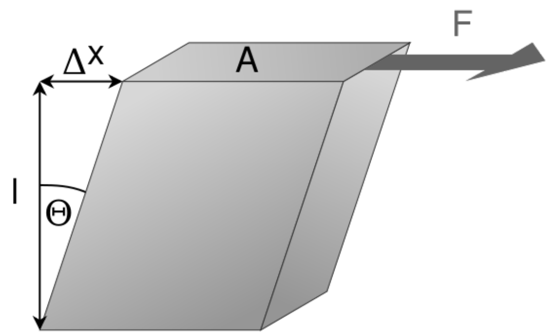

Figure 3.7 Rubber in shear where the plane area, A, is placed under a force, F, creating a displacement Δx at a given angle, θ

As the cords pull away from each other, the rubber between them will experience a shear stress, τ, which can be calculated at a given point as:

$$\tau = \frac{F}{A} \qquad 2$$

This shear stress will produce a displacement Δx or relative to the total length of the rubber s strain, γ, over the total cord length, l:

$$\gamma = \frac{\Delta X}{l} \qquad 3$$

Using the stress and strain values, the modulus of rigidity, G, can be calculated as:

$$G = \frac{\tau}{\gamma} \qquad 4$$

The main limitation in using rubber is that it does not obey Hooke's law for linear isotropic homogeneous materials such as steel or aluminium. This makes it difficult to predict its properties and overall strength. This is compounded further by the fact that each rubber compound will exhibit its own stress vs strain relationship. A new batch of rubber must be tested each time, and its characteristic stress vs strain curve plotted.

Rubber testing and modelling completed by Person and Pickering states that rubber testing conditions should reflect actual operating conditions [12]. Their testing concludes that only loading conditions that match known data sets can be used to predict results in models accurately. Figure 3.8 illustrates the different stress vs strain curves when tested under biaxial, planar and tension loads.

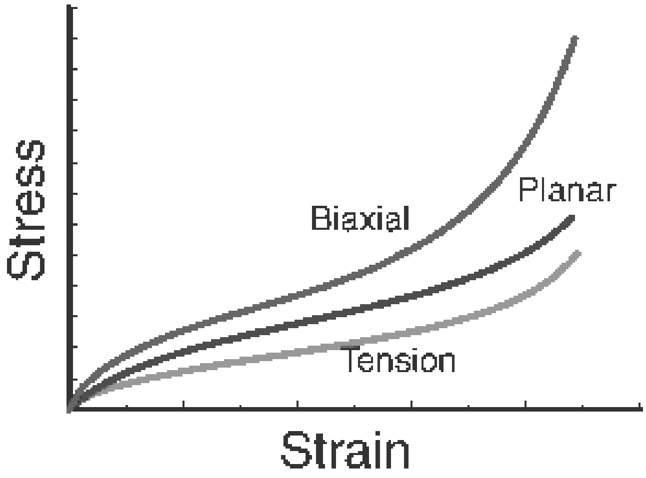

Figure 3.8 Hydrostatic rubber results of uniaxial (tension), biaxial and planar tests [12]

The resultant curves (see Figure 3.8) show how different loading conditions can produce different engineering stresses and strain. If rubber used in a splice was tested only in tension, the model would not reflect the loads applied with sufficiently accuracy. With belt splices, predominantly in shear, a single uniaxial or equibiaxial test will not provide a suitable relationship, and therefore, planar testing would also be required to determine the overall characteristics. Data sets collected from rubber testing are plotted against a curve generated by the general form of the strain energy equation called the modified Mooney Rivlin equation (used for hyperelastic rubber elastomers):

$$\mathrm{W} = \sum_{\mathrm{i=1,j=1}}^{\infty} \mathrm{C_{i,j}}\,(\mathrm{I_1} - 3)^{\mathrm{i}}(\mathrm{I_2} - 3)^{\mathrm{j}} \qquad 5$$

where $C_{i,j}$ are material constants and strain invariants $I_1,\ I_2,\ and\ I_3$ relate to the stored energy in the system. The Mooney Rivlin model is plotted against an experimental stress/strain curve, which allows for the constants to be determined and solving equation 2. By determining the coefficient in this equation, it is possible to determine the rubber shear modulus and hence shear stress.

Predicting rubber properties this way is very accurate, with many journal papers able to make model predictions using FEA. The difficulty comes when trying to determine the strength of a vulcanised splice on site. As discussed previously in the introduction, some of the limitation or difficulties in fabricated splices arise from the vulcanising process itself. Variables such as vulcanising temperature, pressure or quality of equipment affect rubber properties. A conference paper by James on a non-destructive test for belt splices [13] (based on the DIN22131 standard) discusses the use of an edge bar test that produces a duplicate sample of the splice; the samples are then sent for testing to confirm the correct strength was achieved. James' experience suggests that this method is seldom used, likely because of the additional time required to recommission the belt.

Regardless of how much work is done to improve the quality of either fabric or steel cord splices, human factors, conveyor geometry and the environment will always affect the quality and strength of any belt splice. Significant development could be achieved if an alternative method could be utilised for joining conveyor belts.

3.4 Alternative Splicing Bonding Method

An alternative candidate to the vulcanising process would be to use adhesives. These would need to be of high strength, flexible and capable of sustaining structural integrity, even at temperatures up to 80°C. The main contenders for belt splice adhesives are cyanoacrylates (super glue) and epoxy resins. Cyanoacrylates can join two substrates in the presence of moisture 'which is present in small quantities on virtually all surfaces [14], and steel cord and rubber will bond effectively.

The moisture on the substrates allows the polymerisation process to take place, creating a rigid thermoplastic bond. This rigidity causes obvious issues, as it does not allow for flexibility at the joints when under load. Lavoie comments that fully cured cyanoacrylates tend to be brittle, with a minor percent elongation and have low impact strength [14]. Highly flexible cyanoacrylates are now capable of achieving greater than 100% elongation, reducing hardness as show by product A in Figure 3.9 below.

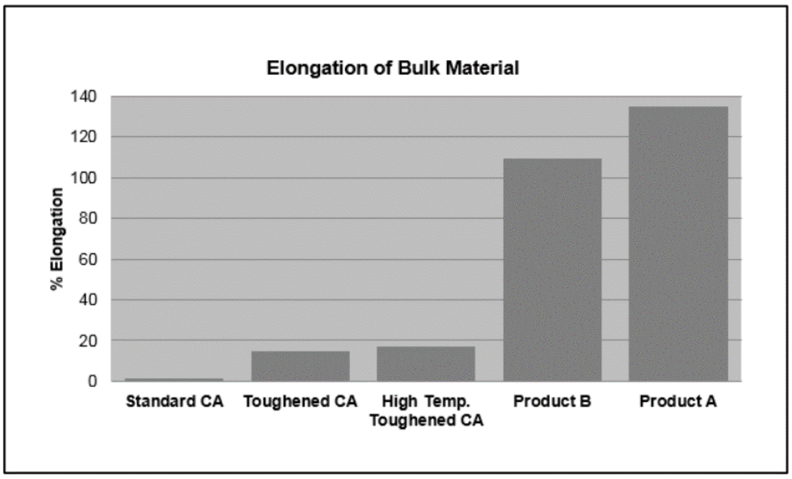

Figure 3.9 Typical cyanoacrylates vs highly flexible cyanoacrylates (Products A & B) [14]

Another issue with cyanoacrylate bonds is that they are thermoplastic and unable to withstand high temperatures; with combined sun radiation and equipment friction, conveyor belt surface temperatures can exceed 60°C, causing bonds to reduce in strength. Typical cyanoacrylates 'can withstand average temperatures of 80°C' [15], but modern cyanoacrylates can now withstand higher average temperatures of 120°C while maintaining more of their tensile/shear strength.

Conveyors in high ambient temperature environments will 'heat age' the bond, potentially reducing its tensile/shear strength by over 50%. This can be seen in Figure 3.10 and Figure 3.11 successively.

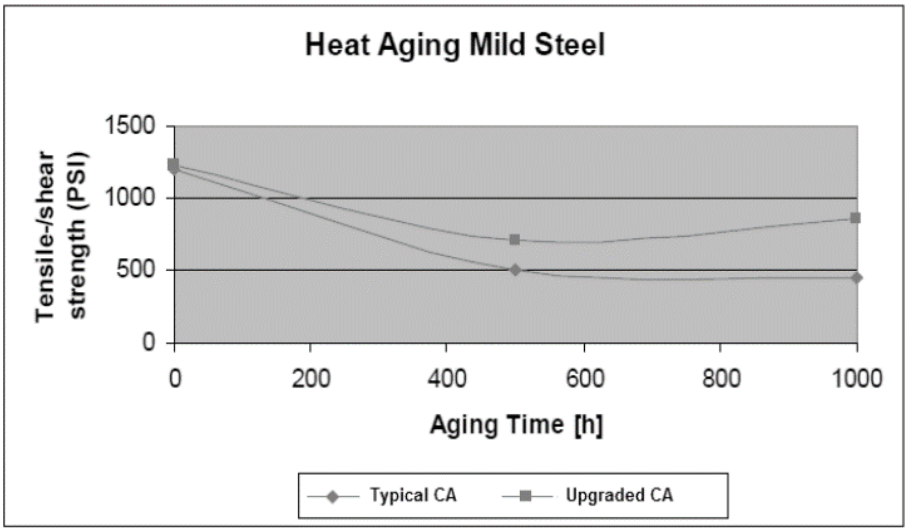

Figure 3.10 Mild steel lap shears assemblies, typical cyanoacrylate heat aged at 80°C and high temperature cyanoacrylate heat aged at 120°C [15]

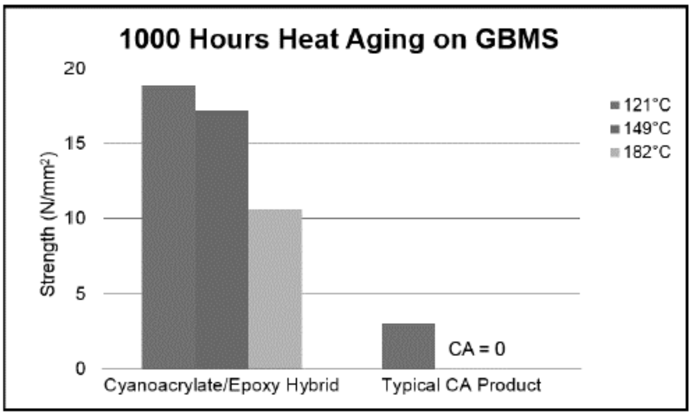

Figure 3.11 Heat resistance of a cyanoacrylate/epoxy hybrid vs a generic cyanoacrylate on grit-blasted steel [14]

By using current-technology super glues, advantages are gained through simplifying construction.

3.4.1 Fixture times

Cyanoacrylates major advantage is a fixture time of seconds, compared with high-strength adhesives, such as epoxy resins, which vary from 15 minutes to 2 hours [14]. Epoxies are adhesives that come in either a single-part or two-part system. In the single-part system, resin and hardener are mixed and hardened, and polymerisation occurs by heating the mixture, creating a thermoset polymer. These are less susceptible to impact and high temperatures. In the two-part system, the resin is mixed and will polymerise at room temperature.

The major limitation in the past has been fixture rates. Lavoie writes that even with additives fast fixture times are normally around 8–15 minutes [14]; this can accumulate to hours considering the amount of cords to be joined in a steel cord belt. Recent adhesive technologies have produced hybrid epoxy/cyanoacrylates that have much quicker fixture times; it is now possible to achieve a zero-gap fixture time of around 180 seconds [14]. Hybrid epoxy/cyanoacrylate adhesives have the best of both properties. They are more resistant to the effects of temperature, more flexible and less susceptible to shrinkage over time. With recent advancements, hybrids perform well against impact and aging, which are critical issues when looking at a suitable splice adhesive, (See Figure 3.12).

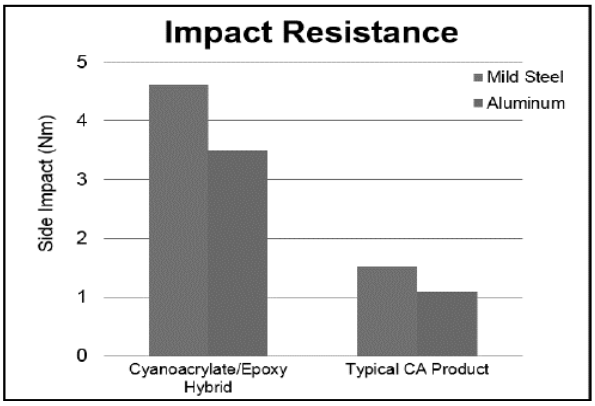

Figure 3.12 Typical impact resistance of a cyanoacrylate/epoxy hybrid vs a generic cyanoacrylate [14]

3.4.2 Curing

Epoxy bonds can take several hours to reach their operating or usable strength.

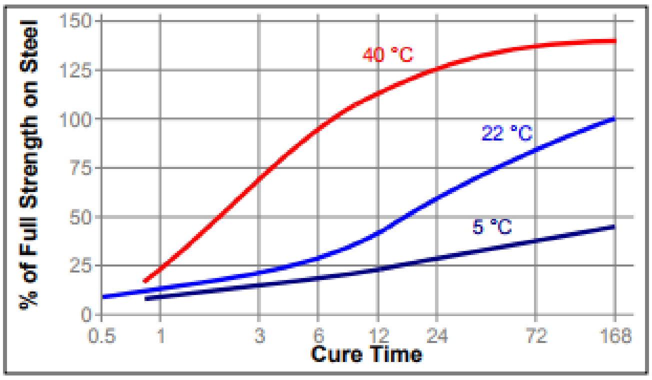

Figure 3.13 Cure speed in hours vs temperature for steel substrates [16]

By increasing the curing temperature of epoxy resin, it is possible to achieve usable strength significantly more quickly. At room temperature (22°C), the strength of a commercial epoxy hybrid adhesive achieves 100% of its strength in 168 hours. By increasing the curing temperature to 40°C, the curing time required to reach 100% strength reduces significantly, to only 6 hours.

A study into the effect of curing conditions on strength development in an epoxy resin for structural strengthening has shown that by increasing curing temperatures to 90°C, it is possible to reduce the curing time from 'several hours at room temperature to approximately 30 mins' [17]. As a rule of thumb, this paper also comments that 'the final strength of the resin is halved for every increase of 10°C in temperature' [17].

3.5 Alternative Concept Development

The development of any new splicing method will require ongoing physical testing in conjunction with computer-aided design. The use of finite element software such as Strand 7 would help increase the speed of any concept development by addressing issues before they are constructed as prototypes. Its main limitation is access to computer processing power. As the model becomes more complex, the number of calculations and iterations increase at a non-linear rate. To reduce the requirements for computer processing time, all efforts were made to simplify the model without affecting its characteristics.

Any proposed alternative splice concept will require modelling contact interaction between the steel wire rope and splice assembly. Steel wire rope is comprised of strands of wire, allowing it to be strong yet flexible. As the steel wire flexes and is placed under load, all the wires that make up the steel wire rope begin to interact with each other. A paper written by Kastratović et al. demonstrates the complexity of modelling the interaction between wires using non-linear frictional contacts (beam contact elements) and linear direct bonding contact (node to node) [18]. The model shown in

Figure 3.14 shows a 7 x 19 construction steel wire, which was used for the FEA. It is comprised of seven strands and 19 wires, all interacting with each other via direct or frictional contacts.

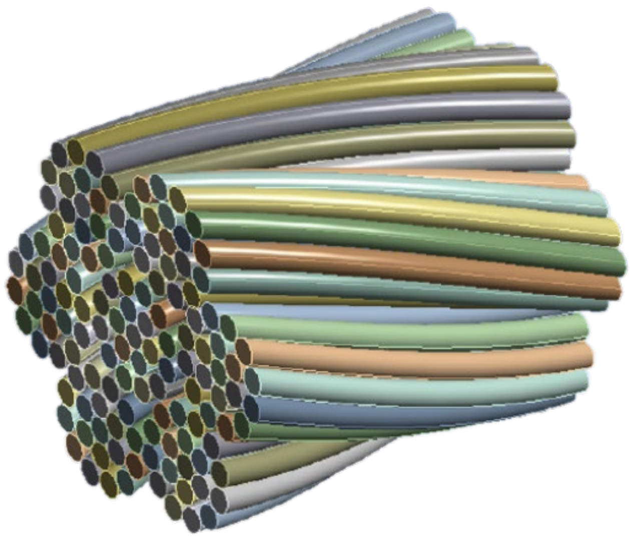

Figure 3.14 7 x 19 steel wire rope construction with each wire and strand bundle modelled [18]

The model was then meshed using 20 node brick elements; in total, the number of bricks used exceeded 329,000 for a 7 x 19 construction steel wire rope only 11 mm long [18], exclusive of the number of frictional contacts required to allow for interaction. Based on previous experience, a standard modern home computer would take at least five days to solve this. In addition, any model would need to rely on estimating the coefficient of friction and Poisson’s ratio. Variation in these two properties could significantly affect any result and would need to be verified through physical laboratory testing.

4 EXPERIMENTAL BASIS

For the basis of the design, static 'pull-out' and full thickness 'tensile strength' tests were conducted for a standard steel cord belt. These tests were carried out as per the Australian Standard AS1334.3. Both the pull-out and tensile strength testing were completed on a tensile test machine (see Figure 4.1).

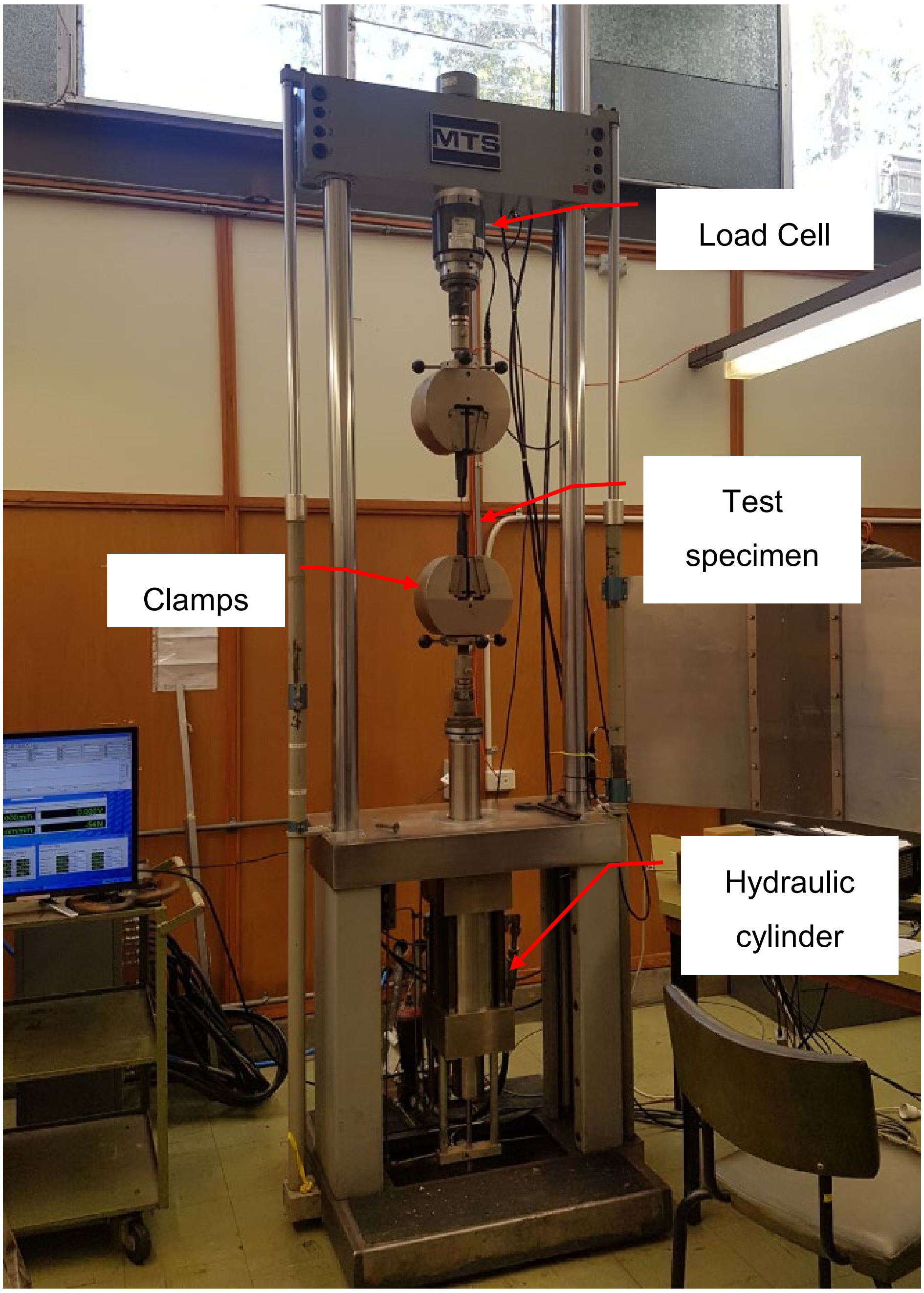

Figure 4.1 MTS tensile testing machine [19]

Compliance requirements specify a minimum allowable pull-out and break cord force for a given belt rating.

Sample conveyor belt specimens are cut to standard dimensions and tested according to Australian Standards AS1333 'Conveyor belting of elastomeric and steel cord construction'. The results are used to confirm the belt rating strength and assess the potential shear strength of the rubber bonded directly to the steel wire rope in the belt.

4.1 Pull-Out Test

The force required to shear a steel cord out of its vulcanised covers is determined by a belt pull-out test and enables us to determine the behaviour of a typical vulcanised splice.

For testing purposes, a Goodyear ST630, 1000 mm wide belt with 10/5 covers was used. The length, L_1, is 50 mm, as specified in AS1333.4.

Figure 4.2 shows the standard dimensions for a belt pull-out test. The samples were cut accurately with tolerance of ±2 mm to comply with Australian Standards.

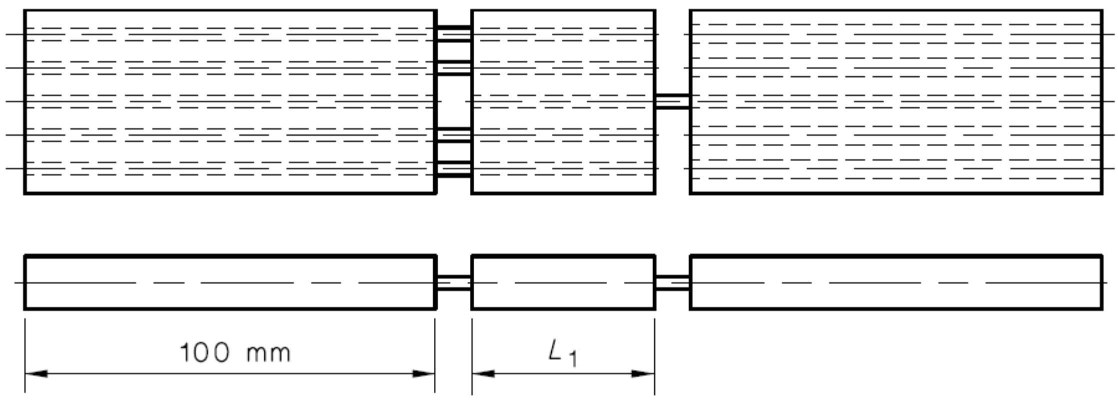

Figure 4.2 Belt pull-out test dimensions as per AS1333

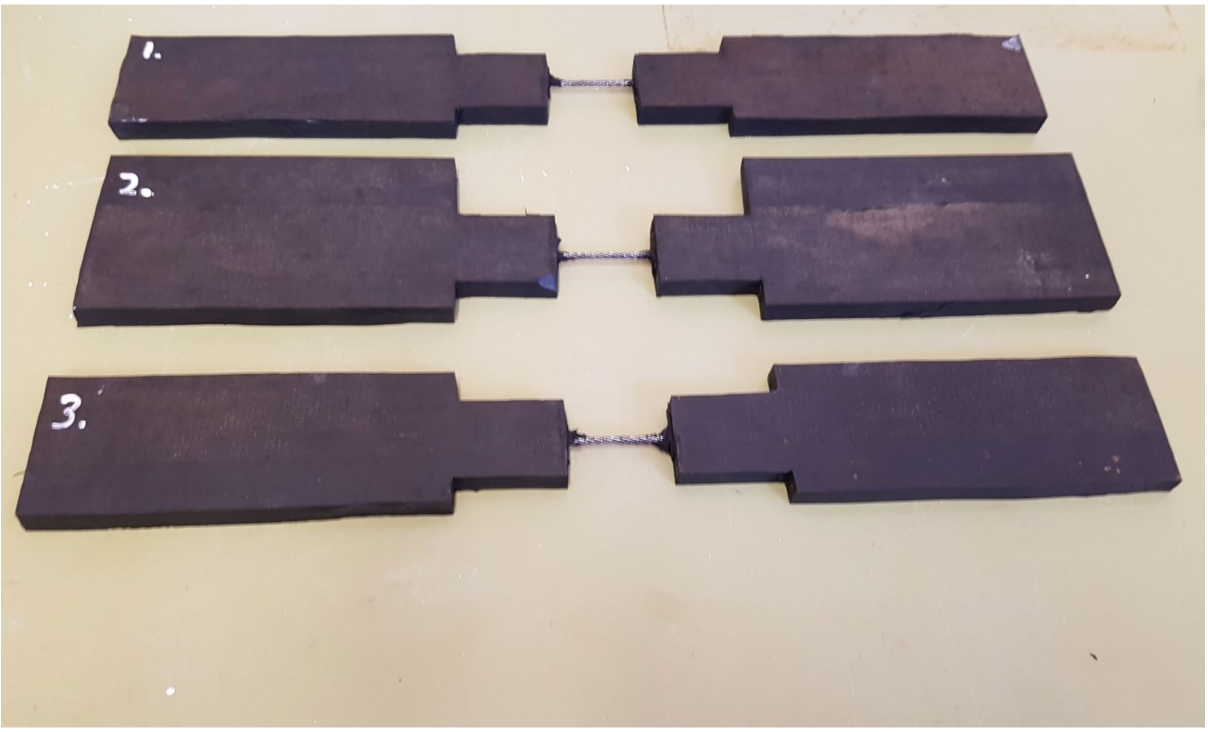

Figure 4.3 ST630 belt pull-out samples as per AS1333 [20]

Three samples were taken—at both ends and the middle of the belt—to ensure a consistent result was recorded throughout the width of the belt. The sample was placed in the tensile testing apparatus, where the computer-controlled hydraulic cylinder applied a separation rate of 100 ± 10 mm/min (as per AS1333).

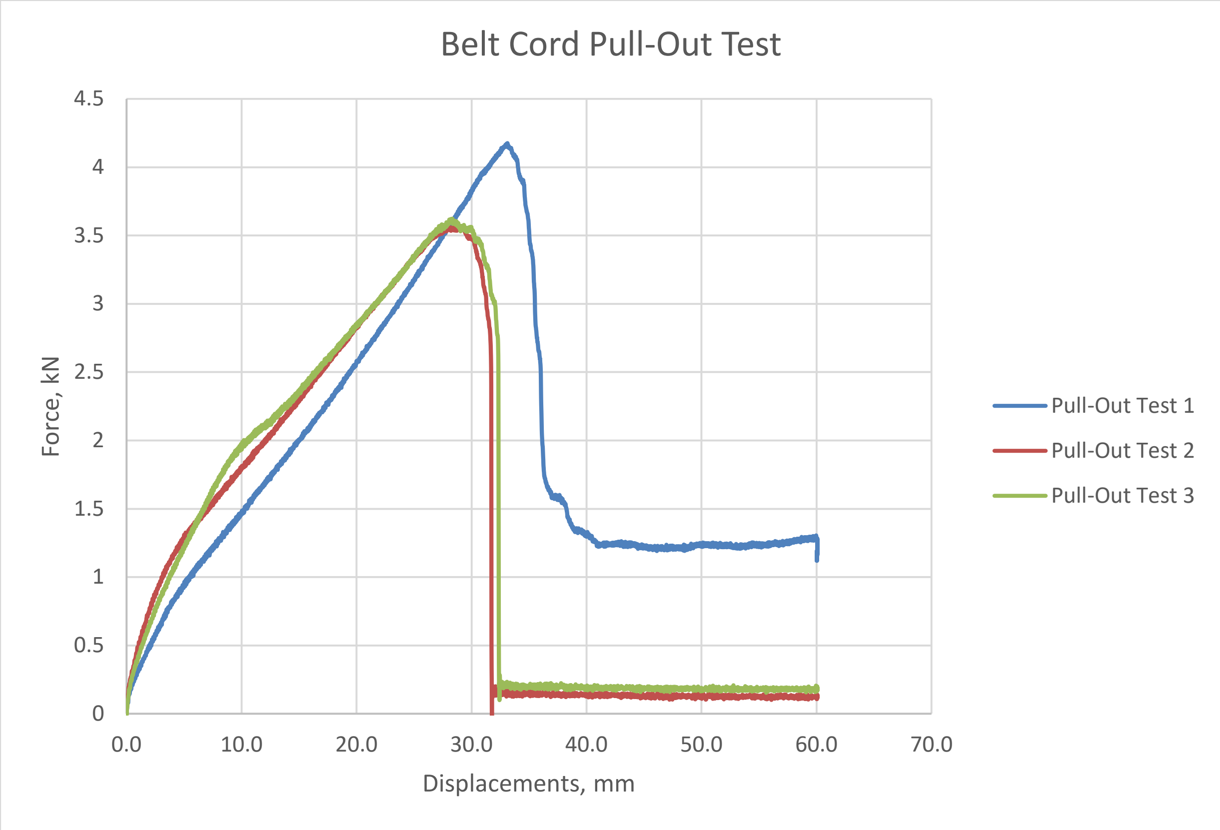

Figure 4.4 Belt cord pull-out results with 100 mm/min strain rate at room temperature

Based on a 100 mm/min separation rate, the rubber for all three tests displaced at a minimum 30 mm before failing (i.e., cord pulling out of rubber).

Figure 4.4 shows that for all three tests, a minimum of 3.5 kN was achieved before failure. This demonstrates consistency in the construction of the vulcanised steel cord belt.

Results from this test provide the pull-out force, F_U, used to calculate 'pull-out' strength P_U in kN/m:

$$\mathrm{P_U} = \frac{\mathrm{F_U} \times 1000}{\mathrm{L_1}} \ (\mathrm{kN/m}) \qquad 6$$

Table 4.1 Unit pull-out test

Based on the AS1333 calculation, the unit pull-out strengths are as follows.

Test	Unit	Result
Pull-out test 1	kN/m	70
Pull-out test 2	kN/m	70
Pull-out test 3	kN/m	82

Note that the minimum pull-out strength (as per AS1333) for a 2.8mm diameter cord is approximately 65 kN/m. Value was estimated from 'Figure 1 Static Pull-Out Strength of Steel Cord' on page 12 of AS1333-1994.

4.2 Cord Break Test

Cord breakage test to determine maximum strength at failure was also conducted. Three test specimens again were cut out from the sides and middle of the belt and placed into the MTS tensile test machine.

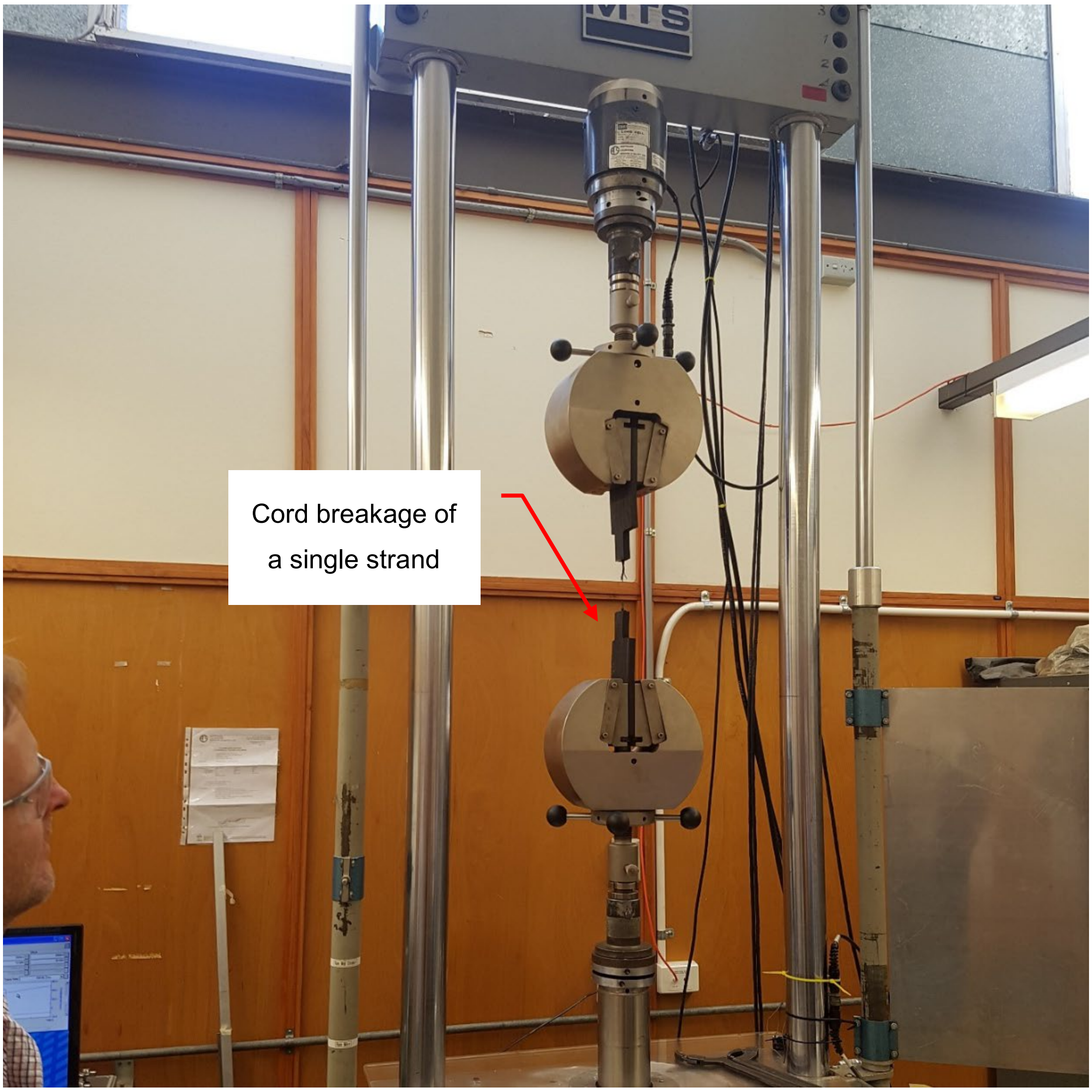

Figure 4.5 Cord breakage test

Results were collected tabulated and summerised in Figure 4.2.

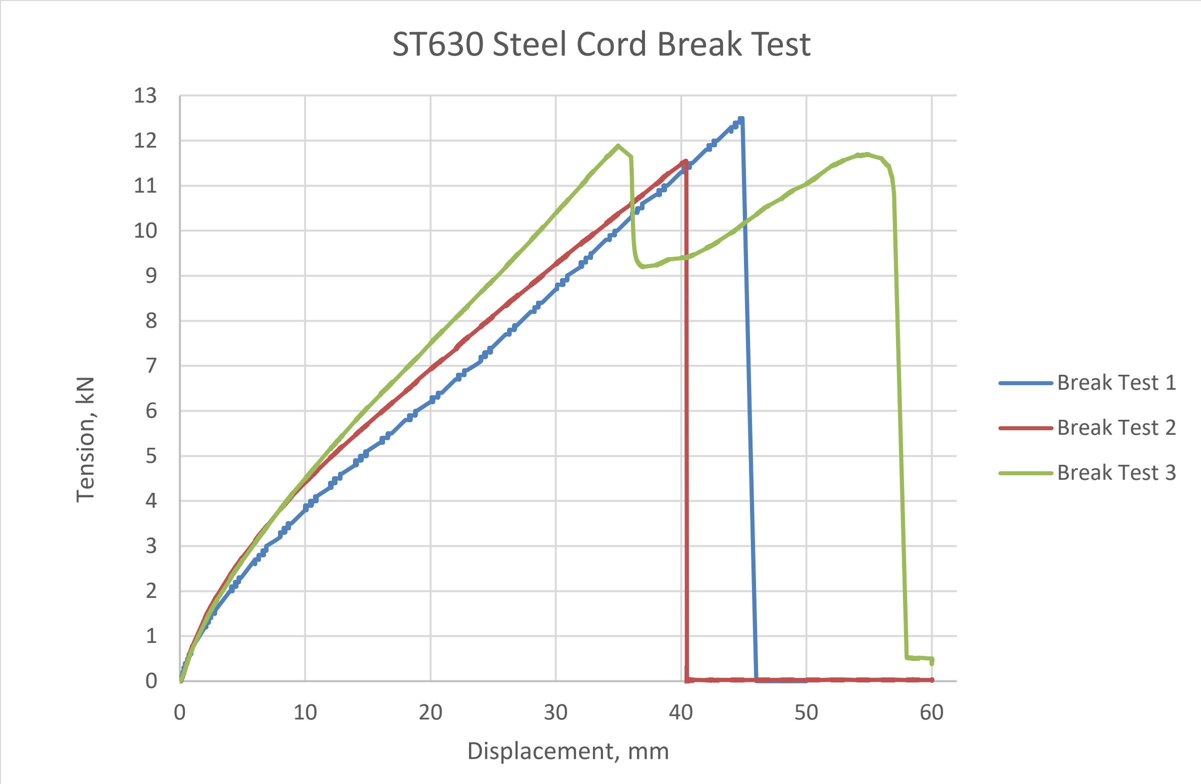

Figure 4.6 ST630 steel cord break test, cord diameter 2.8 mm cord dia. with a 50 mm/min strain rate at room temperature

Table 1 'Designation and suggested parameters of conveyor belting of elastomeric and steel cord construction' in [21] shows that minimum allowable breaking strength for a ST630 cord is 8.2 kN

Table 4.2 Tensile test cord breakage test for 2.8 mm diameter steel wire rope

Test	**Unit**	**Result**
Breakage test 1	kN	12.5
Breakage test 2	kN	11.5
Breakage test 3	kN	11.8

All three break tests exceed the minimum allowable breaking force by 20%, which would mostly like allow for manufacturing errors or mistreatment of the conveyor belt during normal operations.

It should be noted that only static testing was conducted. These tests were conducted for baseline data, which can be used as a reference when reviewing data from our concept splice assembly results.

5 SPLICE ASSEMBLY CONCEPT

Current splicing technology requires the splicer to successfully join both steel cord and fabric conveyor belts together. A skilled crew working in an ideal environment will be able to construct either a steel or fabric belt splice to manufacturer's requirements; however, experience suggests that these conditions are seldom achieved. Though true for both fabric and steel cord belt splice construction, this work focuses on providing a method to address environmental and construction issues. A new design will need to use minimal components and have a simplified construction methodology that reduces the chance of splice failure due to poor workmanship. A new splice assembly method (Figure 5.1) is proposed, which aims to address current issues affecting strength and longevity. This new assembly is comprised of three types of components utilising mechanical threading, friction and adhesive bonding to connect steel wire ends together to provide a strong and flexible join.

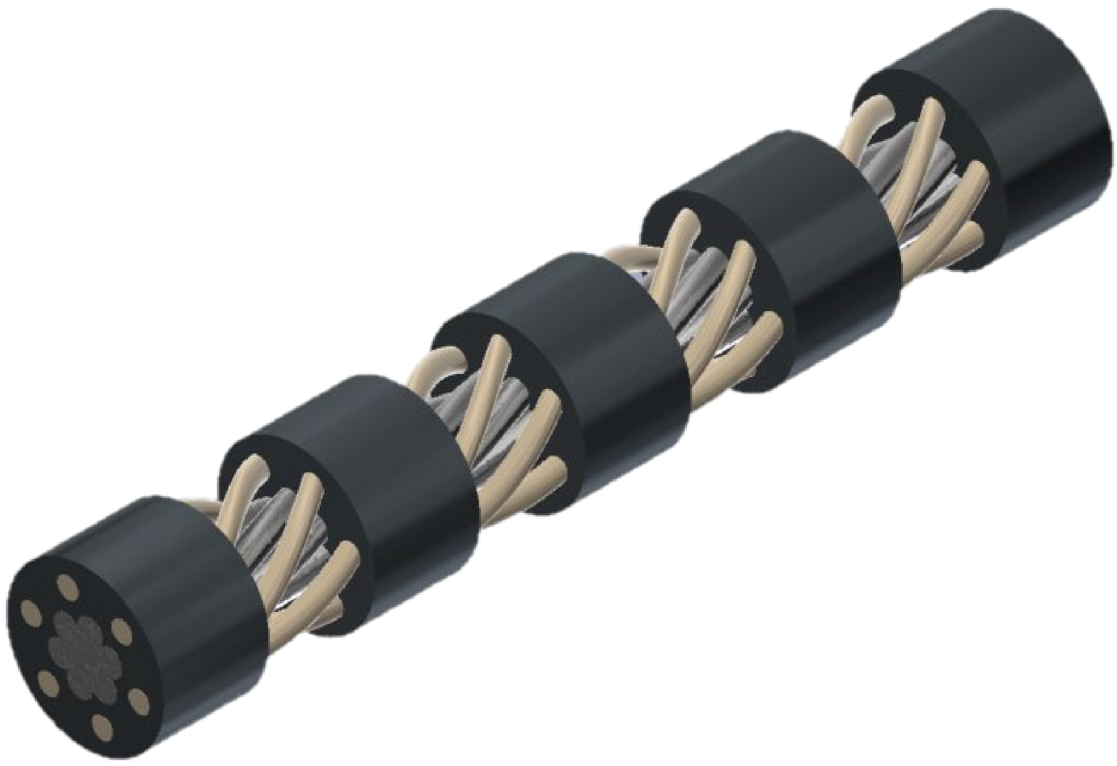

Figure 5.1 Splice assembly concept

The number of ferrules and diameter of connecting wires will vary depending on steel cord belt rating.

The assembly is made up of three main components (see Figure 5.2 and Table 5.1 Splice assembly component summary table

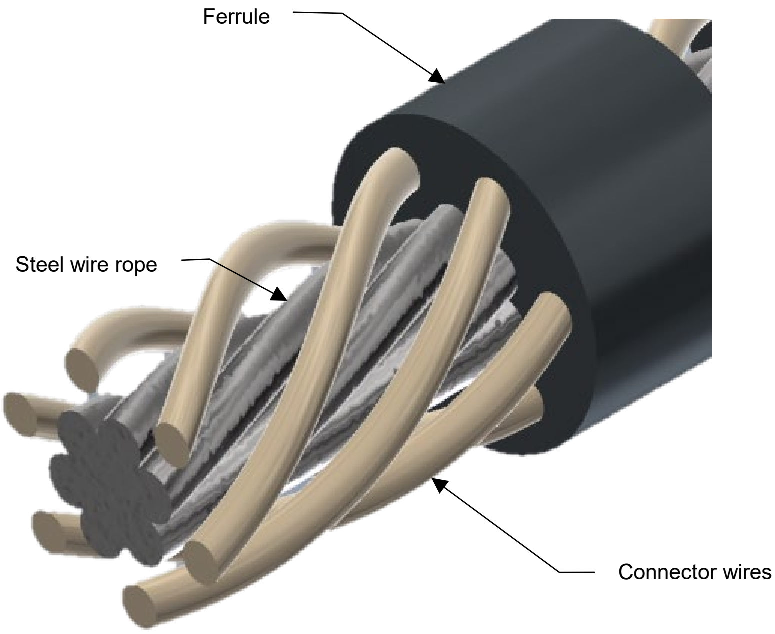

Figure 5.2 Assembly components

Table 5.1 Splice assembly component summary table

Component		Ferrule Connector Wire	
Property		A4 - AISI 316SS	
Type		7x7 construction	
Dia.	mm	1	
Area	mm^2	0.785	
Minimum Breaking Load	N	610	
Minimum Tensile Stress	N/mm^2	777	
Component		Ferrule	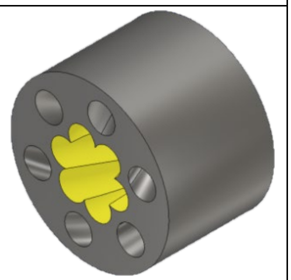
Property		EOS SS GP1	
Type		3D meter printed	
Ultimate Tensile Strength	MPa	980	
Yield Strength	MPa	500	
Component		Conveyor belt steel wire rope	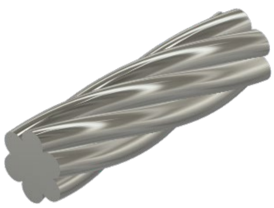
Property		EEEIP	
Type		7x7 construction	
Area.	mm^2	3.53	
Minimum Breaking Load	N	8400	
Minimum Tensile Stress	N/mm^2	2160	

Ferrule connector wire rope selection was based on availability; however, material could change to mild steel.

3D printing of the ferrule limits the type of construction material to either stainless steel or titanium. Stainless steel was selected as it is approximately three times cheaper than titanium. If the assembly was put into mass production, it would also likely be made of a readily available mild steel.

The properties of the steel wire rope used in the conveyor belt can only be estimated as this information is not made available by the manufacturers. Assembly substrates are bonded together by a high-strength structural epoxy/acrylic adhesive.

The ferrule (Figure 5.3) has a helical bore, which allows it to mechanically thread itself onto the steel wire rope. The helical bore and outer holes also share the same pitch and should allow the splice assembly to achieve continuity between steel wire ends.

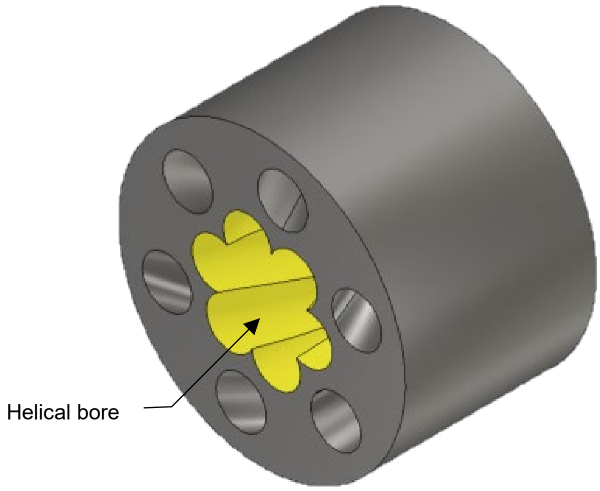

Figure 5.3 Ferrule with helical bore and outer holes

The helical shape inside of the ferrule provides an internal thread, allowing the steel wire rope to screw in (see Figure 5.4).

Figure 5.4 Section of connector with steel wire rope threaded

Steel wire rope is comprised of numerous wires and strands; however, it can be simplified by smoothing the outer edges (see Figure 5.5).

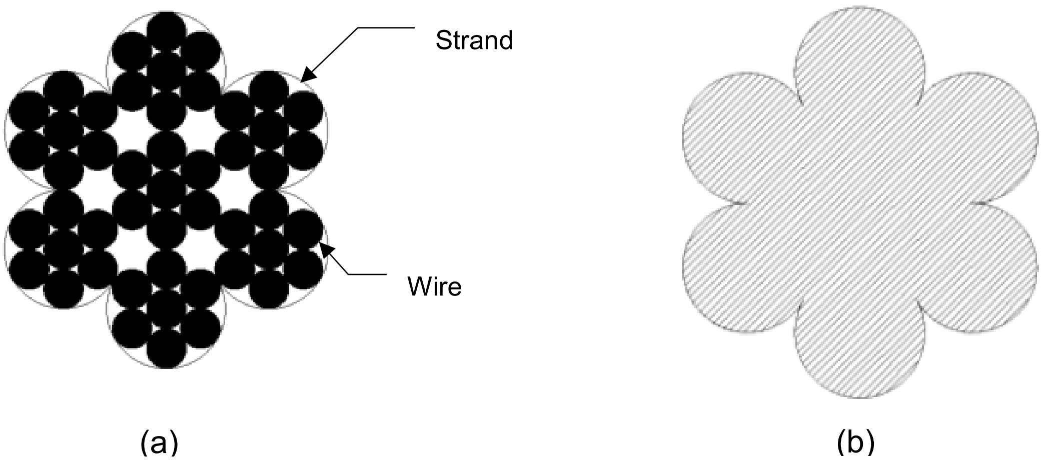

Figure 5.5 Steel wire rope; (a) typical 7 x 7 steel wire rope cross section, (b) simplified steel wire rope cross section

As the steel wire rope threads through, segments of each strand are in contact with the ferrule helical bore. Each segment (see Figure 5.6(a)) has a cross-sectional area that supports axial load.

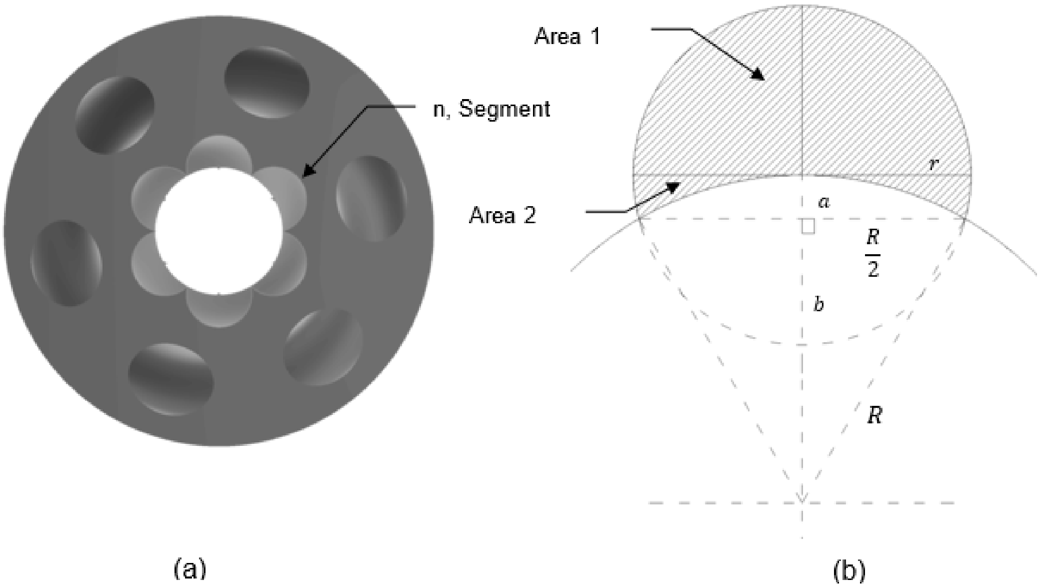

Figure 5.6 SWR and ferrule contact area; (a) ferrule cross section, (b) SWR segment contact area

The number of segments is determined by the type of steel wire used; for example, the ST630 belt uses a 7 x 7 strand construction, which has six outer strands and one inner (core). Each of the outer strands produces a segment when viewed as a cross section (see Figure 5.6(b). This segment is in contact with the inside of the ferrule, it will resist axial loading and torsion (steel wire rope will twist under axial load).

The hatched area can be determined as follows. Small radius, r can be calculated using Pythagoras' theorem where:

$$\mathrm{r} = \sqrt{\mathrm{a}^2 + \left(\frac{\mathrm{R}}{2}\right)^2} \qquad 7$$

And

$$\mathrm{R}^2 = \left(\frac{\mathrm{R}}{2}\right)^2 + \mathrm{b}^2 \qquad 8$$

Rearranging for b we get:

$$\mathrm{b} = \frac{\mathrm{R}\sqrt{3}}{2} \qquad 9$$

Also,

$$R = \frac{R\sqrt{3}}{2} + a \tag{10}$$

$$a = R - \frac{R\sqrt{3}}{2} \tag{11}$$

Substitute a into equation 6 we get:

$$r = \sqrt{\left(R - \frac{R\sqrt{3}}{2}\right)^2 + \left(\frac{R}{2}\right)^2} \tag{12}$$

Therefore, area 1 can be calculated by:

$$A_1 = \frac{\pi}{2}\left(\left(R - \frac{R\sqrt{3}}{2}\right)^2 + \left(\frac{R}{2}\right)^2\right) \tag{13}$$

Area 2 can be approximated by:

$$y = -\frac{a}{r}x^2 \tag{14}$$

$$A_2 = -\int_{-r}^{r} \frac{a}{r}x^2 dx \tag{15}$$

$$A_2 = \frac{h}{3r}x^3\Big]_{-r}^{r} \tag{16}$$

The total amount of steel wire rope in contact with the ferrule is the tensile stress area A_T, calculated via:

$$A_T = n[A_1 + A_2] \tag{17}$$

Where n is the number of steel wire rope segment in contact with a ferrule.

A 7 x 7 steel wire rope configuration with six outer segments (see Figure 5.6) will have the equivalent of one full segment in contact when threaded into the ferrule with one-sixth rotation. Therefore, all six segments will be in contact with the ferrule after one full rotation. For example, for a ST630 steel cord belt with 7 x 7 wire rope configuration and a 25 mm 'thread pitch', one full ration would mean that six segments (analogous to threads) are in contact.

A ferrule (analogous to a nut) is 5 mm wide with a 25 mm internal thread pitch. This mean that after one full rotation, six segments have engaged approximately 5 mm of thread, for a total equivalent thread engagement of 30 mm per ferrule.

During axial loading of the splice assemblies, each ferrule will be placed in shear, due to the small threads inside the ferrule, there is a potential for shearing to be the main cause of failure. The ferrule internal shear stress area A_s can be approximated as follows

$$\mathrm{A}_s = \mathrm{PCD} \times \mathrm{L} \tag{18}$$

Where L is the length and P is the pitch circle diameter as shown in Figure 5.7 below,

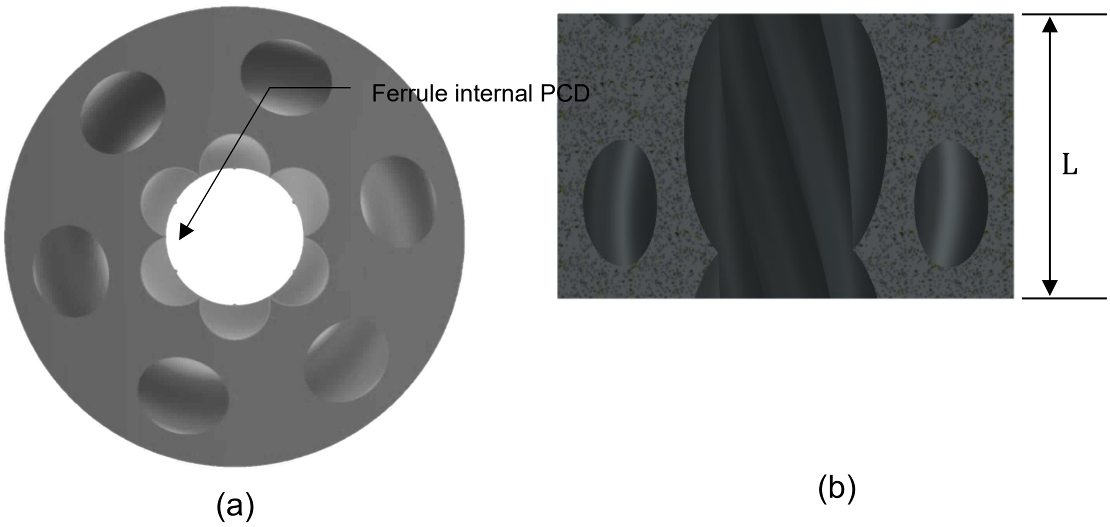

Figure 5.7 Ferrule; (a) ferrule PCD, (b) ferrule length, L

Cross-sections a and b above show the ferrule can be considered analogous to a threaded nut which can screw on the helical shaped steel wire rope.

The contact area between ferrule and connecting (refer to Figure 5.8) wire will create a friction force when under axial loading.

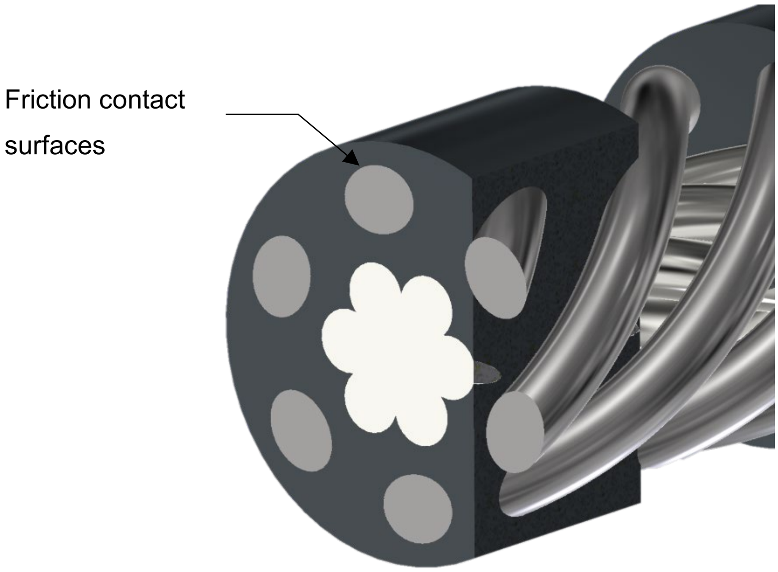

Figure 5.8 Ferrule and connecting wire contact

Friction force between ferrule and connecting wire can be approximated by:

$$F = \mu F_N \quad (19)$$

where μ is the coefficient of friction and F_N is the force normal to the contact surface.

The coefficient of friction for steel-to-steel contact can be determined through experimentation, and can vary with material condition, temperature and moisture content, among others. Connections between steel wire rope/ferrule and ferrule/connector components will be bonded with an adhesive to resist twisting when the steel wire rope is under load.

5.1 Assembly Method

The splice assembly installation method is practical enough that each steel cord can be spliced together in one minute, not including preparation. Therefore, a metre-wide ST630 steel cord belt with over 40 cords may take less than an hour to complete. Prior to assembly, each cord must be cleaned and most of the rubber removed. Imbedded rubber inside the cord should not affect bonding between surfaces.

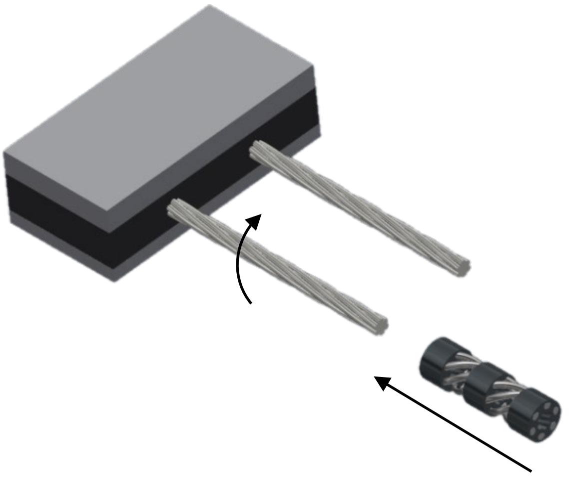

Figure 5.9 Stage 1 – Apply adhesive to SWR and screw one side in first

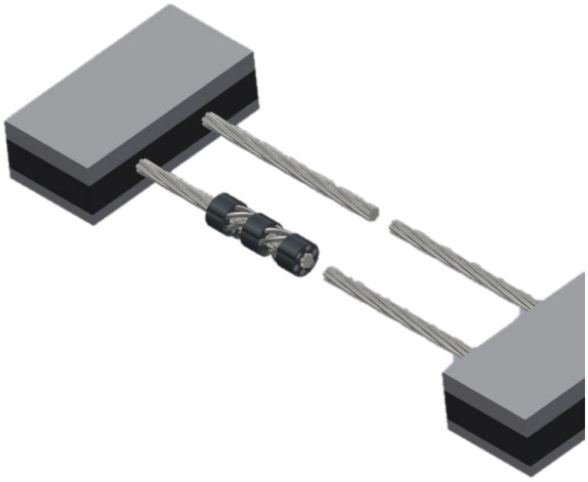

Figure 5.10 Stage 2 – Over screw one side and bring pairing cords together

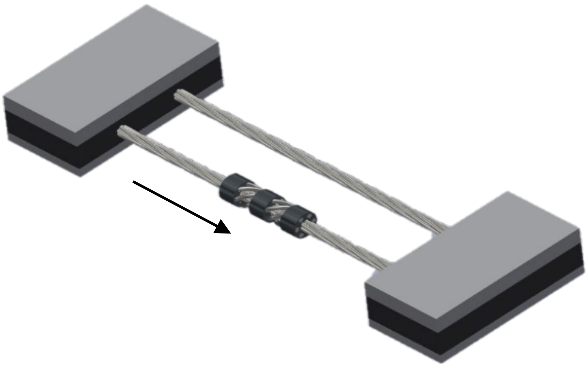

Figure 5.11 Stage 3 – Splice assembly is then back screwed to pairing cord to complete the assembly

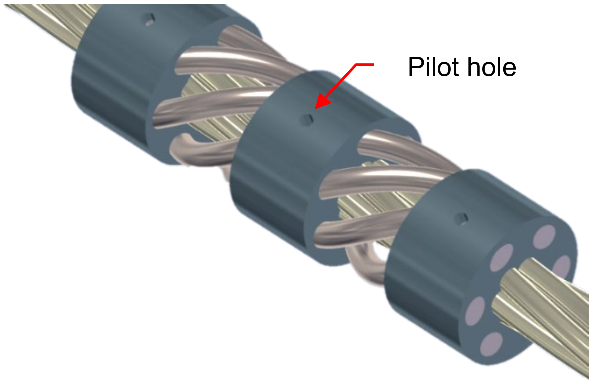

Figure 5.12 Stage 4 – Adhesive can be added through the pilot holes in each ferrule

Once all cords are paired and spliced, a quick-setting flexible polyurethane or acrylic can be used to fill gaps between cords. Alternatively, a standard method of using strips can also be used. The purpose of looking at different options to bind the splice assembly together is to reduce the amount of time to construct the splice, as well as preventing the splice from twisting. Figure 5.13 below shows a typical exploded splice using proposed ferrule splice assembly.

Figure 5.13 Splice assembly with top and bottom moulded covers (exploded isometric view)

Moulded vulcanised top and bottom covers will be bonded together using the same hybrid adhesive used to join splice assembly. Because of the helical construction of steel wire rope, when placed in tension, it will naturally want to twist. This will in turn transfer torsion to the splice assembly. The connector cable will be exposed to combined stresses including tension, torsion, shear and bending. The splice assembly along with top and bottom splice covers will be bonded together using commercially available structural adhesives meeting the following criteria:

- Adhesive must be strong but sufficiently flexible to sustain cyclic loading
- Manual handling of adhesive can be done safely with minimal personal protection equipment (PPE)
- Bonding is required to be different substrates (e.g., rubber and steel or rubber and fabrics)
- Working strength must be achieved within three hours to reduce conveyor downtime

- Adhesive must work effectively even when exposed to high ambient temperatures.

5.2 Test Assembly Construction

Physical construction was difficult due to the size of each ferrule assembly. Figure 5.14 illustrates a 6mm diameter 3D printed stainless steel ferrule used for the prototype splice assemblies.

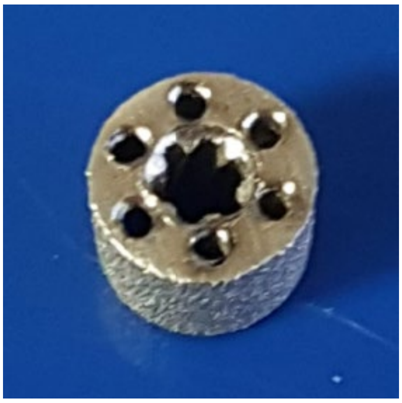

Figure 5.14 3D printed ferrule assembly

All ferrule holes were cleaned and edges bevelled to allow for insertion of steel wire rope. This was quite labour intensive, with each ferrule taking approximately ten minutes to prepare. From here, ferrule connector wires are inserted (Figure 5.15)

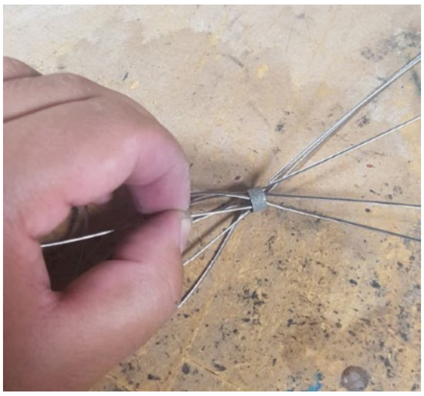

Figure 5.15 Connector wires being inserted

Once all the ferrule connector wires are inserted and glued together, splice assemblies of any length can be made. Figure 5.16 below shows a completed five ferrule assembly followed by insertion on to 2.8mm diameter steel wire rope.

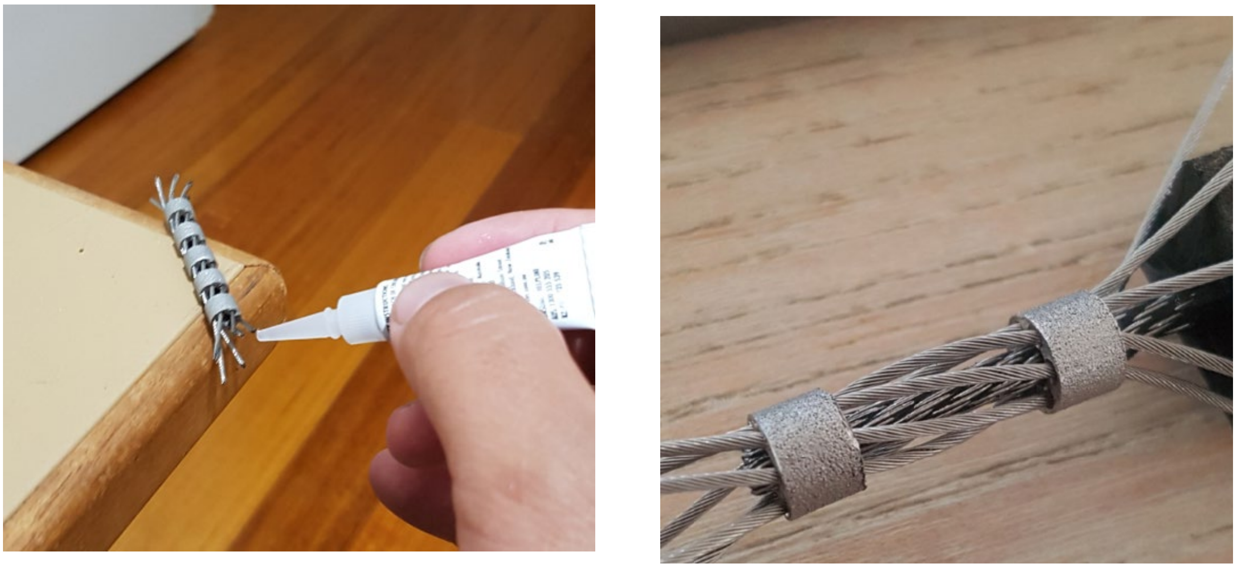

(a) (b)

Figure 5.16 Splice assembly; a.) Complete assembly being glued together, b.) Splice being screwed on to steel wire rope

The completed assembly with steel wire ropes screwed in shown in Figure 5.17 below.

Figure 5.17 Completed five ferrule splice assembly used for MTS tensile test machine

Creating a splice assembly is very time consuming with each one taking approximately six hours to complete. This was mainly due limited available tools, poor ferrule production properties and a lot of trial and error constructing a first of its kind assembly. Further development is required; however, it is foreseeable that practical automated method could be conceived to produce these assemblies in mass.

Refer to Appendix A “Operators Splice Manual” regarding detail on assembly concept splicing methodology.

6 ASSEMBLY VERIFICATION

A computation method has been used to verify laboratory tensile testing of proposed splice assembly.

6.1 FEA verification model

FEA was used to predict the stresses on the proposed splice assembly while under axial load. Because of the geometric complexity and number of brick elements required, only three-ferrule assemblies were modelled (see

Figure 6.1 and Figure 6.2).

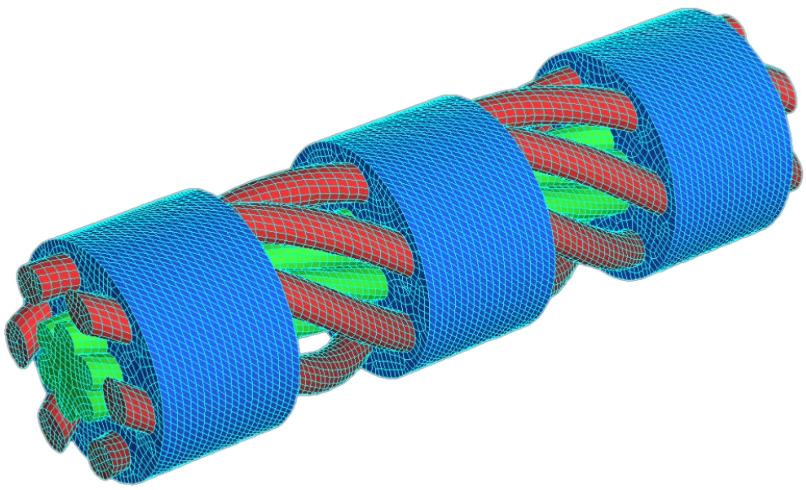

Figure 6.1 Three ferrule finite element model with ferrule connectors and steel wire rope in the same direction of rotation.

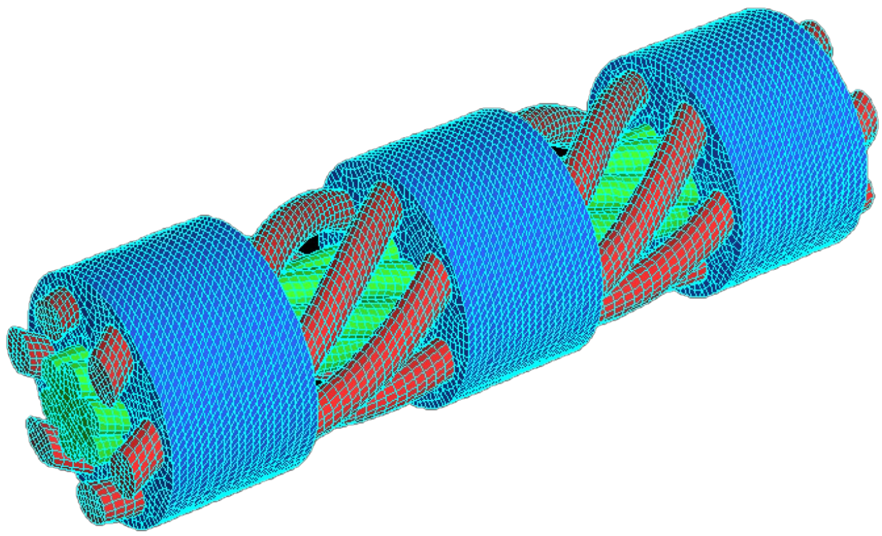

Figure 6.2 Three-ferrule finite element model with ferrule connectors and steel wire rope in opposing direction of rotation

As discussed in the literature review, the splice assembly was simplified by modelling steel wire as a solid and not a weave of wires and strands as shown in Figure 6.3.

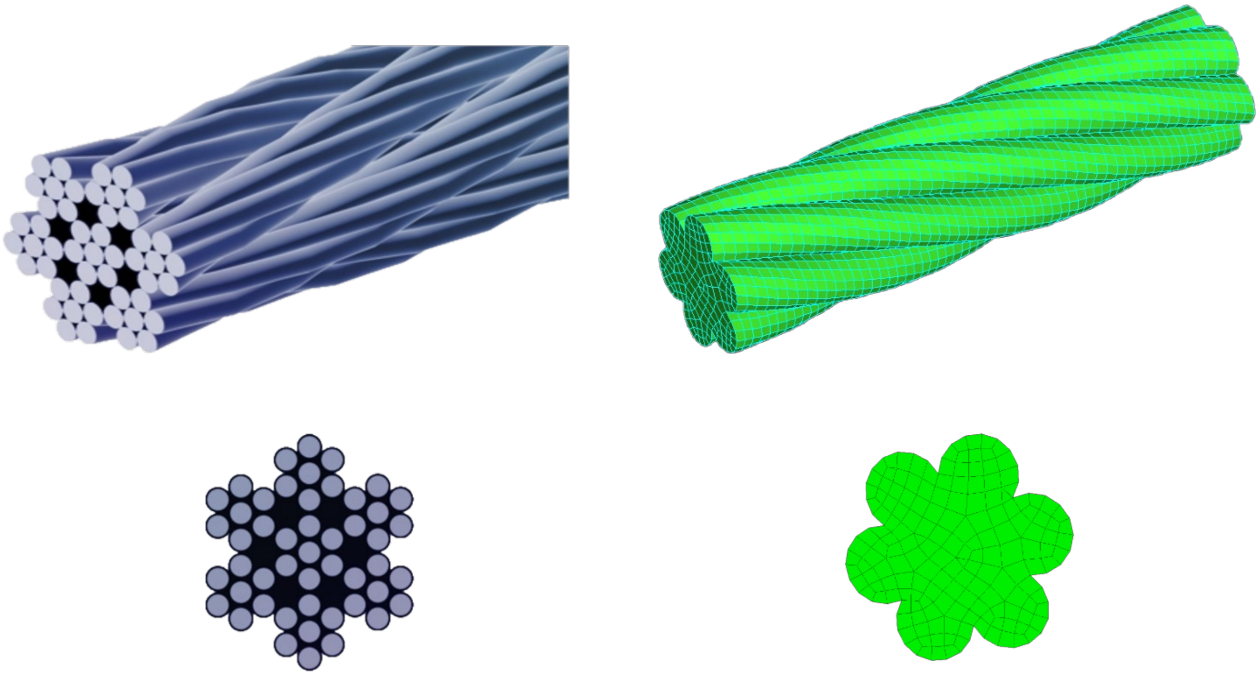

(a) (b)

Figure 6.3 Steel wire rope assembly; (a) 7 x 7 construction steel wire rope showing all 49 wires in bundles of seven wires, (b) finite element brick model with solid geometry

This approach brings challenges, as the steel wire rope acts differently to a solid. Unlike a solid bar, steel wire rope will tend to twist, reduce in diameter and elongate (without yielding) while under load. With testing and ongoing development, it is possible to develop a solid wire model that emulates the characteristics of actual wire rope. To estimate the effects of elongation, a slightly higher Poisson ratio was used. Kastratović et al. [18] and Wenzheng et al. [22] both use a Poisson ratio of 0.3 for their similar 1 x 7 and 1 x 19 construction steel wire rope analysis. As a basis for this analysis, an initial estimate of 0.35 was used. Further work is required to verify this assumption.

The splice assembly models use thousands of 8-node hexahedral bricks and point contact frictional elements. A summary of elements is shown in Table 6.1.

Table 6.1 Elements used in the construction of FEA splice assembly

Assembly	Element	Qty	Use
Inline	Hexahedral (8 node brick element)	69,996	Component stress
	Point contact (friction contact)	6,802	Friction
Opposing			
	Hexahedral (8-node brick element)	71,746	Component stress
	Point contact (friction contact)	6,802	Friction

Because of the large number of elements, each model can take 7–9 hours to solve on a 32-bit system. Future solving software will utilise 64-bit systems, allowing solving time to decrease significantly.

Load transfer from steel wire rope to ferrule is determined by direct node-to-node contact of hexahedral brick elements (see Figure 6.4).

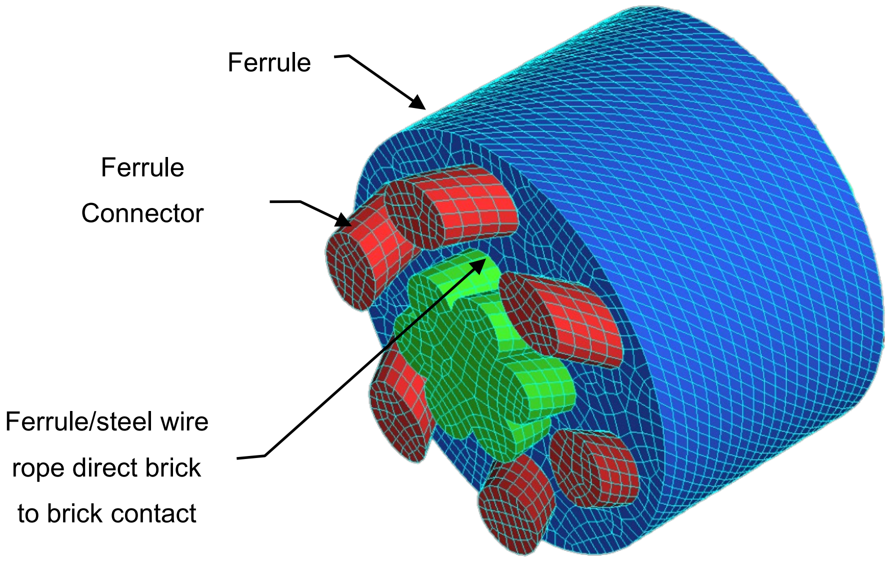

Figure 6.4 Node-to-node contact between steel wire rope and ferrule

Interaction between ferrule and ferrule connectors is determined using a non-dimensional contact beam element (point contacts) to join each component node to node (see Figure 6.5).

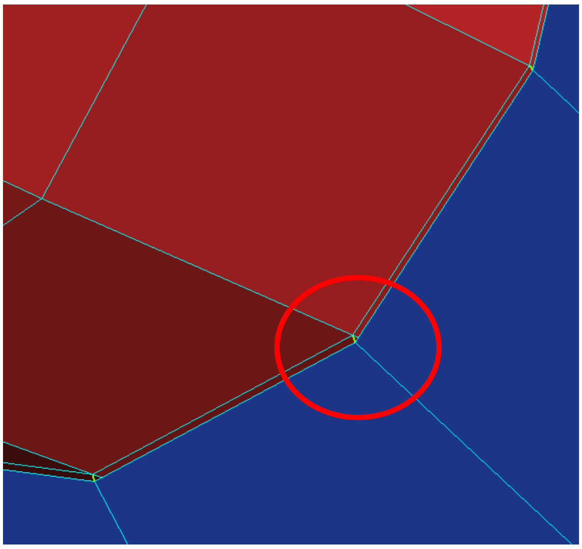

Figure 6.5 Point contact (in light green) between ferrule and connecting wires

Contact beam element properties allows a friction coefficient to be defined between the ferrule and connector wire; additional loads are only calculated when point contacts are in compression. Figure 6.6 shows the point contact beam cloud joining ferrule and ferrule connector wire.

The FEA uses a rectangular yield surface model that predicts frictional behaviour independent of each other. The maximum calculated frictional force becomes the axial load applied (F) times the respective coefficient of friction (μ). Strand 7 defines these as follows:

$$V_1 = \pm F\mu_1 \qquad (20)$$

$$V_2 = \pm F\mu_2$$

Where V_1 and V_2 are frictional forces in two principal directions [23].

For the basis of this investigation, a value of 0.5 was used for the coefficient of friction as there is rough steel-to-steel contact between ferrule and ferrule connectors. Like the proposed Poisson ratio, this is only a best estimate based on industry experience, and further testing is needed to confirm this value.

Figure 6.6 illustrates the point cloud cluster used to connect ferrule and ferrule connector wires.

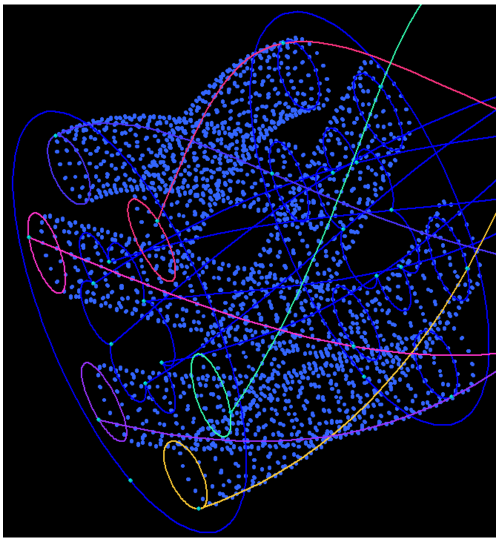

Figure 6.6 Point contact cluster connecting ferrule and ferrule wire connector

6.2 Results Summary

An axial load of 3.6kN was applied to the splice assembly finite element model below. A summary of loads below are based on Figure 6.7 for an assembly with ferrule connectors and ferrules in opposing directions.

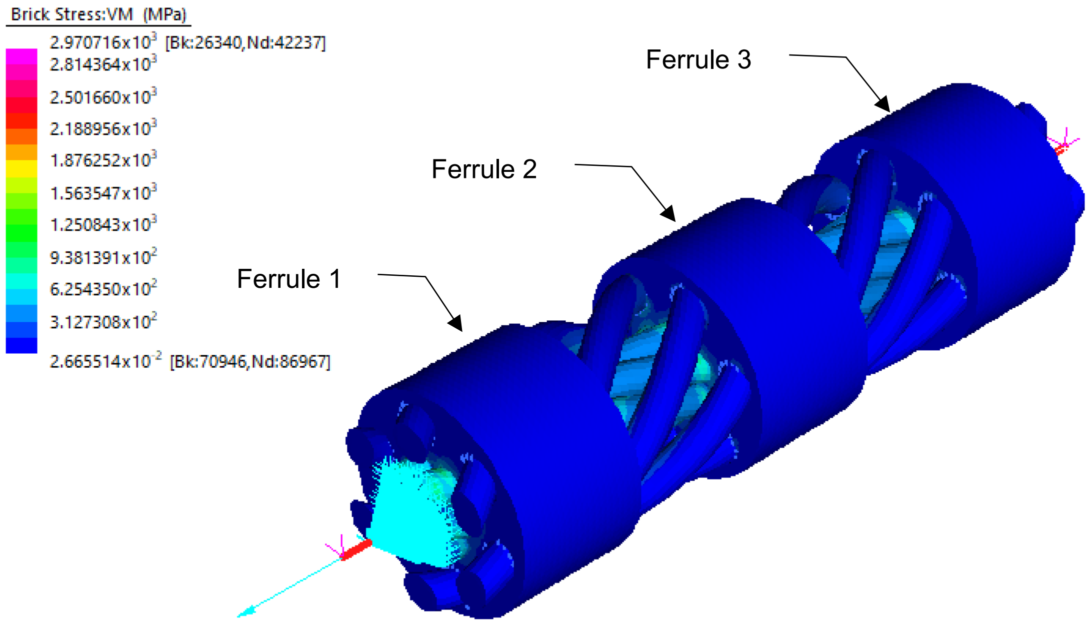

Figure 6.7 Von Misses Stress for splices assembly

Figure 6.8, Figure 6.9 and Figure 6.10below illustrates tensile stress through the steel wire rope at all three ferrule locations under an applied axial load of 3.6kN.

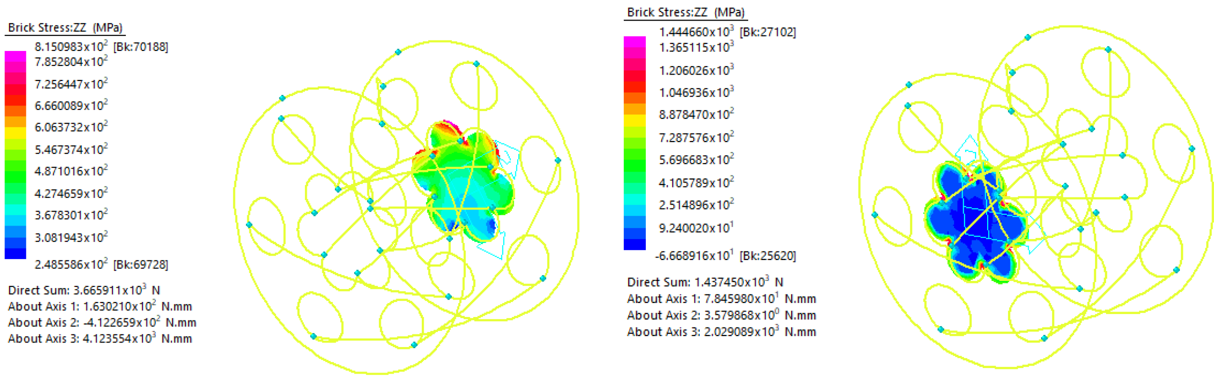

(a) (b)

Figure 6.8 Ferrule 2; (a) left side, (b) right side

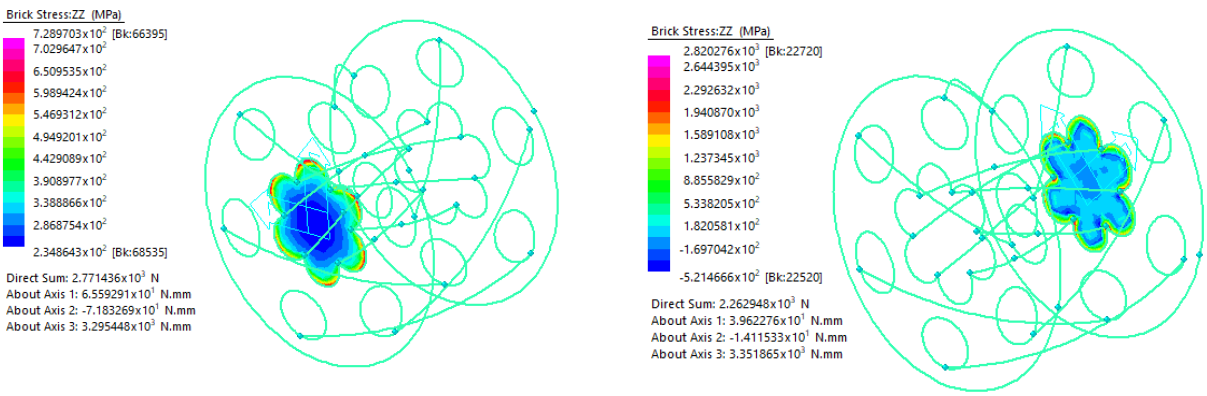

(a) (b)

Figure 6.9 Ferrule 1; (a) right side, (b) left side

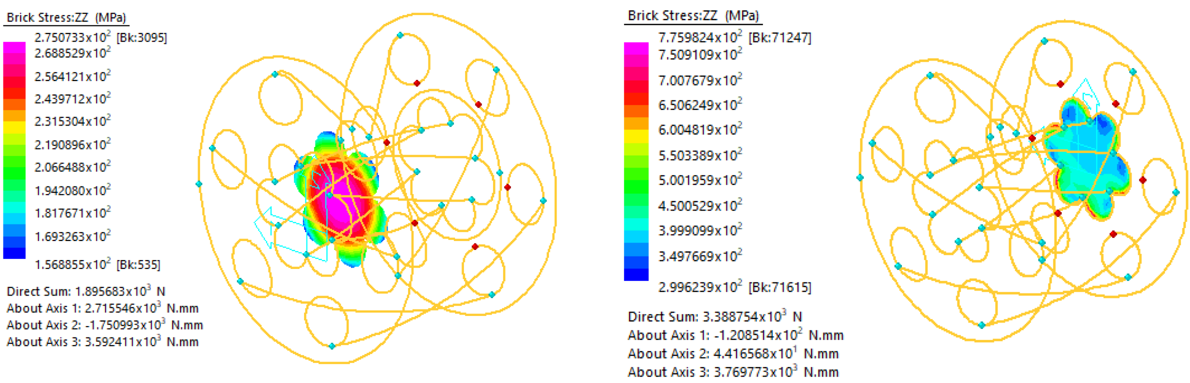

(a) (b)

Figure 6.10 Ferrule 3; (a) left side, (b) right side

Results from Figure 6.8, Figure 6.9 and Figure 6.10, indicate that the splice assembly does not distribute load evenly along the section in contact with it. Summary of loads at each ferrule (Figure 6.11) shows that load is not distributed evenly.

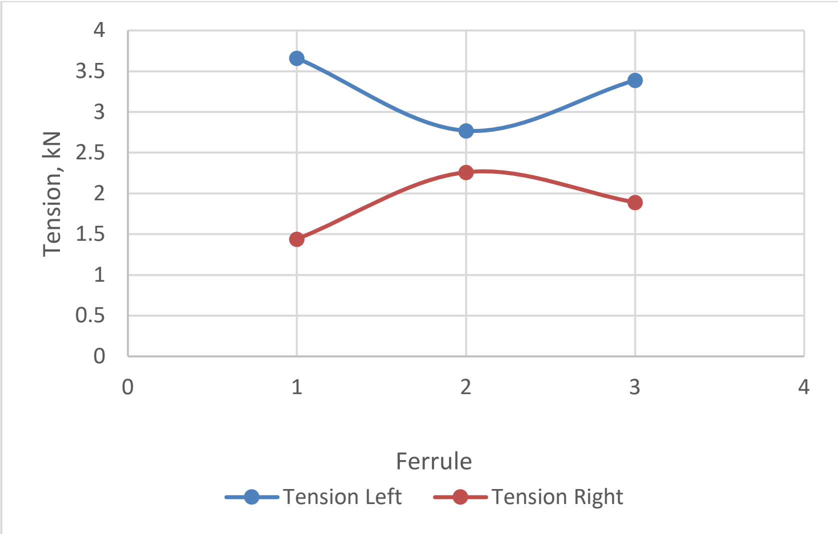

Figure 6.11 Load differential between ferrules under axial load

Figure 6.11 shows a load differential between both (left and right) sides of the ferrule, that is due to the helical profile of the steel wire rope. The symmetry of both plots indicate that tensions will equalise at the middle ferrule and will also observe little to no torsion. This uneven load distribution between ferrule means that outer ferrules of any assembly will be under greatest load (both tension and torsion). Future splice assembly designs will need to take this to account by considering both, a modified geometry and material selection.

Additionally, this torsion creates an abnormal stress concentration (singularities) as shown as red in both Figure 6.8 and Figure 6.9. All sharp edges on the ferrule are bevelled before construction therefore these singularities should not occur. By neglecting these singularities, an even load distribution can be seen by a green boundary around the wire indicating a tensile stress ranging between 600MPa and 815MPa, since this is less than its minimum breaking strength of a 2160MPa failure is not predicted to occur.

Each ferrule is under both tension and shear therefore combined stresses are considered. Figure 6.12 summarises Von Mises stress below.

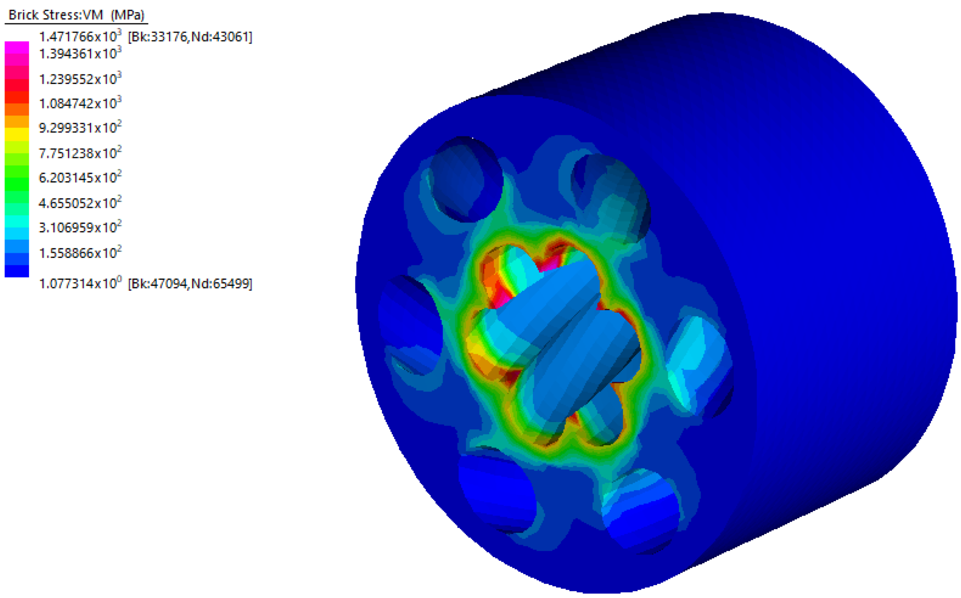

Figure 6.12 Ferrule Von Mises stress from a three-ferrule assembly

Again, these stress concentrations (shown in red above) do not realistically emulate the contact with the steel wire rope and can be disregarded i.e. bevelled edges. Regardless, the evenly distributed yellow and green bands are still high and exceed 900 MPa and would likely cause the ferrule to potentially fail under shear. Stresses could be reduced by increasing the number of ferrules in the system or constructed from a high-yield material such as titanium. It is likely that more ferrules would be used in an assembly to reduce stresses, as it is possible to make a high volume of mild steel parts cheaply compared with making them out of titanium. As mentioned previously, edges will be bevelled in area where it will be in contact with steel wire rope.

Ferrule are joined together with smaller diameter steel wire rope, with the rope resisting tension with a combination of a minor amount of adhesive and friction. Again, this wire will be under a combined load of tensile stress, torsion and bending, therefore Von Mises stress has been considered and is shown in Figure 6.13 below.

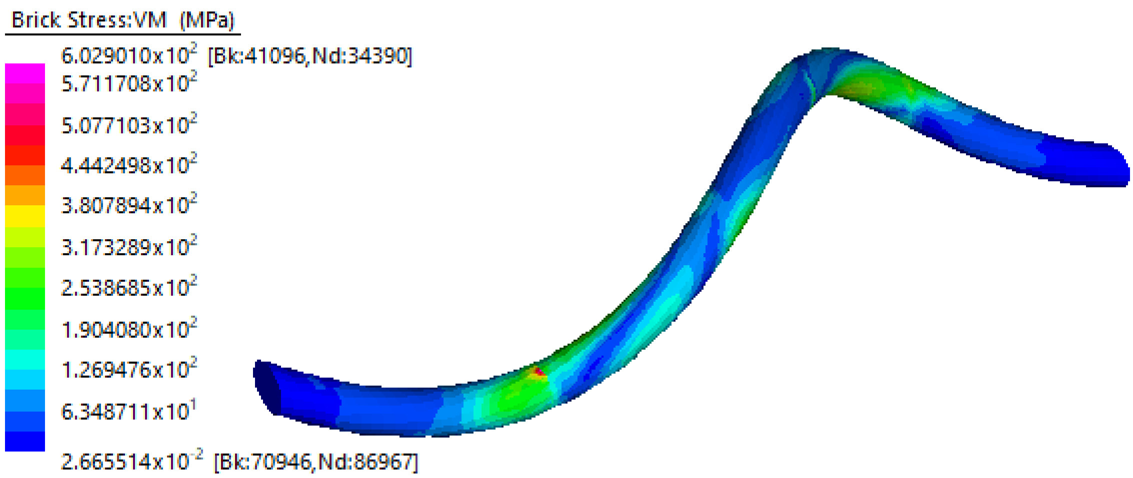

Figure 6.13 Von Misses Stresses for ferrule connector wire (1mm diameter steel wire rope)

Again, there is a small stress singularity where the wire contacts the ferrule edge. As with the other components this is not considered. With a 3.6kN axial load applied to the splice assembly, there is a possibility that these ferrule connector wires might fail considering that even with the singularity stresses may approach 400MPa. For the assembly to a sustain higher loads, a high tensile wire would be needed.

To sustain load using friction, ferrule connector wires apply a downward load on the ferrule as shown in Figure 6.14 below.

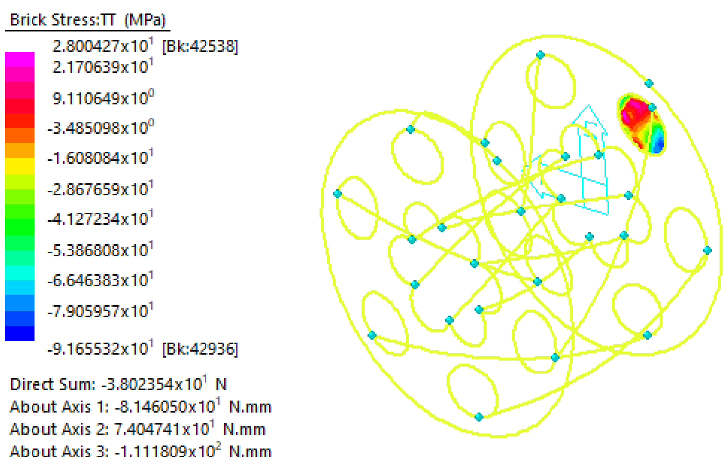

Figure 6.14 Ferrule Connector Compressive Loads on ferrule

The load summary indicates each ferrule connector can apply approximately 38N which equates to approximately 228N per ferrule. Based on a co-efficient of 0.5 and only three ferrule it will only have a resistance of 342N (excluding the resistance from adhesive) against axial load. Again, with the exclusion of the adhesive, thirty-six ferrules would be needed to support the load of 3.66kN or 74 ferrules to achieve 8.4kN. Obviously, the adhesive will have a significant impact and it is likely that a lot less ferrules would be required. Additionally, ferrule connector wire pitch could change to increase normal load on the ferrules. The effects of adhesive and change of pitch would need to be studied in more detail in future investigations.

Refer to Appendix B “Finite Element Model Construction” regarding the process used to develop Strand 7 assembly model.

7 SPLICE ASSEMBLY TESTING

Validity of the splice assembly concept was tested using the University of Newcastle MTS machine, as discussed in Chapter 4. Steel cord belts use various diameter wires; however, it is possible to validate the use of the splice assembly concept by only testing the smallest diameter commercially available (e.g., the 2.8 mm steel wire rope used in the ST630 conveyor belt [6]). All material used for the splice assembly has linear properties; this allows the assembly to be scaled for larger diameter steel wire rope. The main limitation affecting splice assembly is minimum size; by constructing a prototype for the smallest diameter steel wire rope, constructability can be validated.

The minimum breaking strength for the 2.8 mm diameter steel wire rope used for the conveyor belt is 8.4 kN when a strain rate of 50 mm/min is applied [24]. Because of limited resources, the splice assemblies used in testing were constructed using steel wire rope with a lower rating for ferrule connectors. Future assemblies will utilise a much stronger wire and additional connector wires, to achieve the required strength rating.

All tests used a 7 x 7 construction, 1 mm diameter marine grade 316 stainless steel wires with a rating of 510–610N (this varies widely depending on the manufacturer). By using six wires (see Figure 7.1), each splice assembly has a combined breaking strength of approximately 3.6 kN (excluding the reduced rating due to unforeseen stress concentration while under load).

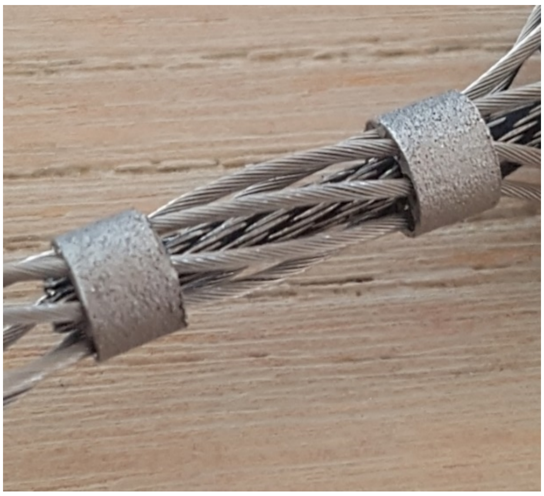

Figure 7.1 Section of splice assembly with 7 x 7 construction, 1 mm diameter steel wire rope (external)

Each splice assembly will have 150 mm length of rubber cover on each side to ensure sufficient clamping pressure can be applied and prevent slipping.

Figure 7.2 Typical splice assembly with rubber cover either side to allow for sufficient clamping force

Test samples are placed in the tensile test machine (see Figure 7.3).

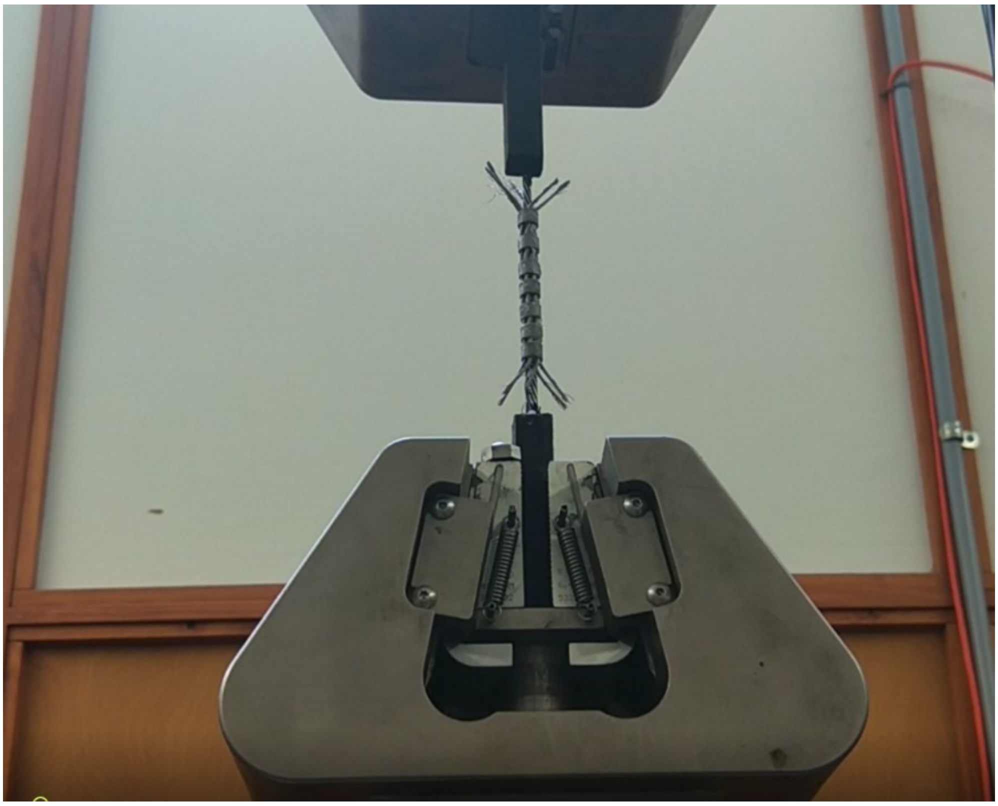

Figure 7.3 Splice assembly under tension in MTS machine

Two design variations of the splice assembly concept were tested to determine which could potentially reduce stress on the wire while holding maximum load:

- Variation one has ferrule connector wires and steel wire rope with a 25 mm pitch with the same direction of rotation as shown in Figure 7.4a.
- Variation two has ferrule connector wires and SWR with 25 mm pitch in opposing direction of rotation as shown in Figure 7.4b.

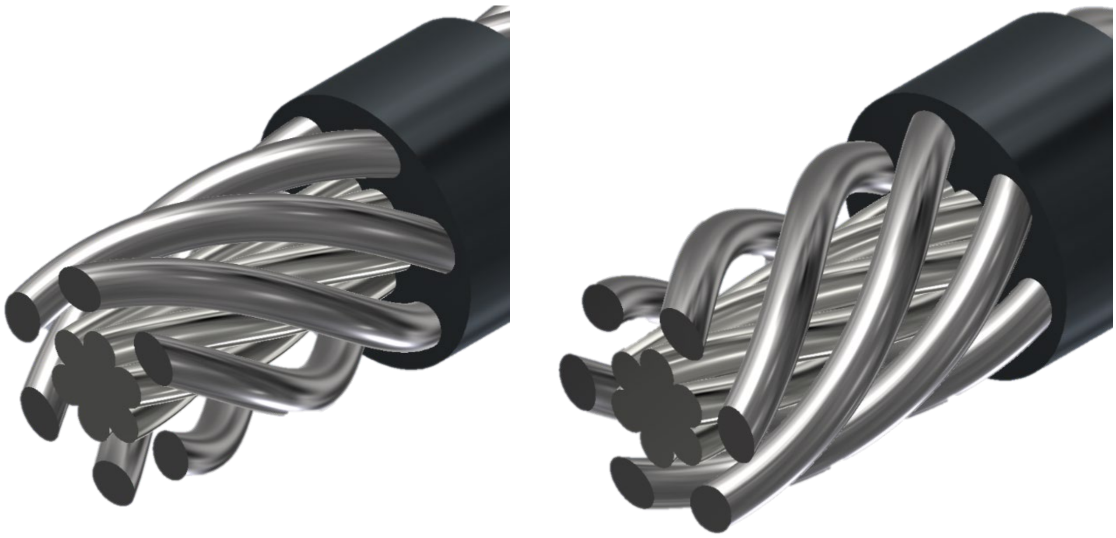

(a) (b)

Figure 7.4 Splice assembly variations; (a) ferrule connector wire and SWR with same direction of pitch, (b) ferrule connector wire and SWR with opposing direction of pitch

In total, six assemblies were constructed, with three having the same direction and three opposing directions of pitch. Additionally, each assembly comprises different quantities of ferrules, ranging from 7–11 ferrules per assembly (see Table 7.1).

Table 7.1 Summary of ferrule assemblies tested

No. of ferrules per assembly	
Same direction of rotation	Opposing direction of rotation
7	7
9	9
11	11

7.1 MTS Tensile Test Results

As previously discussed, an applied strain rate of 50 mm/min was applied to each assembly. Tensile stress over time was measured, with the data collated, plotted and summarised below.

Figure 7.5 shows test results of a seven-ferrule splice assembly. Connector wires and steel wire rope pitch share the same direction of rotation.

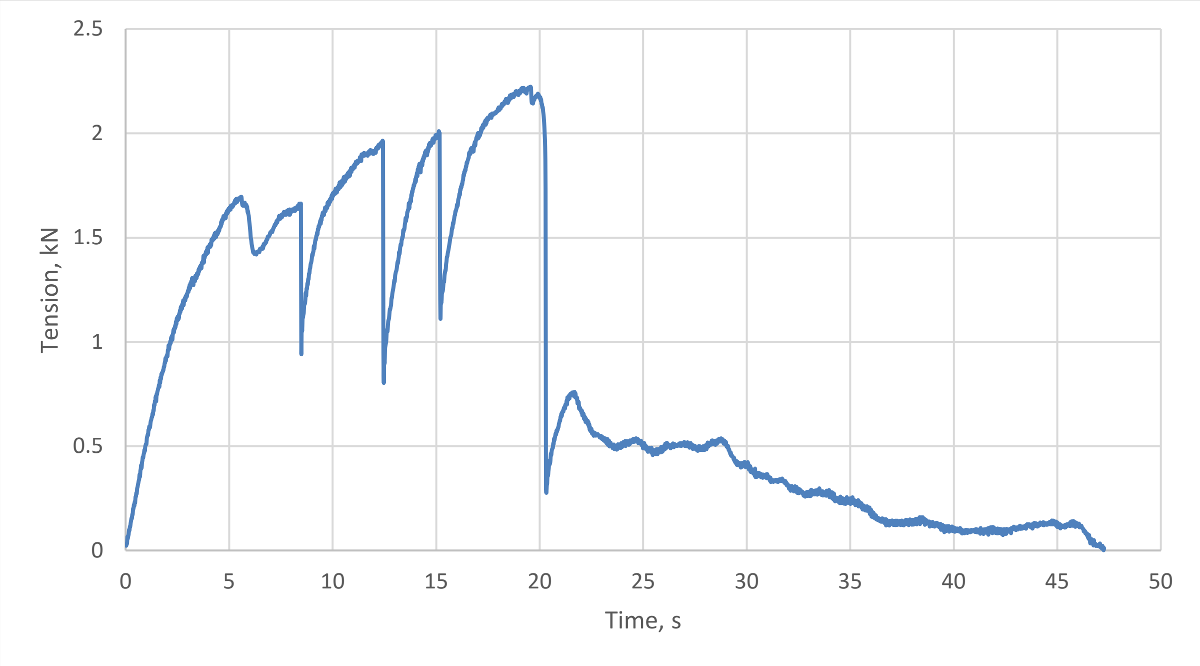

Figure 7.5 Splice assembly, seven-ferrule connector wire and SWR with same direction of rotation

Figure 7.5 shows that the maximum tension was reached at just over 2.18 kN from there, the cyanoacrylate adhesive bonding ferrules and steel wire rope fail due to increasing torsion. After 12 seconds, there is a small enough strain to unwind the ferrules from the steel wire rope. The assembly only failed because of a lack of adhesive strength; no ferrule nor ferrule connector were shown to have signs of failure. Ferrules' 25 mm internal pitch thread were also intact, with no signs of shearing. Test video shows the whole splice assembly twisting 60–90 degrees before failure. Additionally, only the bottom section of the assembly failed, indicating that the bonding application process was not adequate (i.e., quality of preparation and environment).

The sequence shown in Figure 7.6 is for a seven-ferrule assembly. Connector wire and steel wire rope have the same direction of rotation.

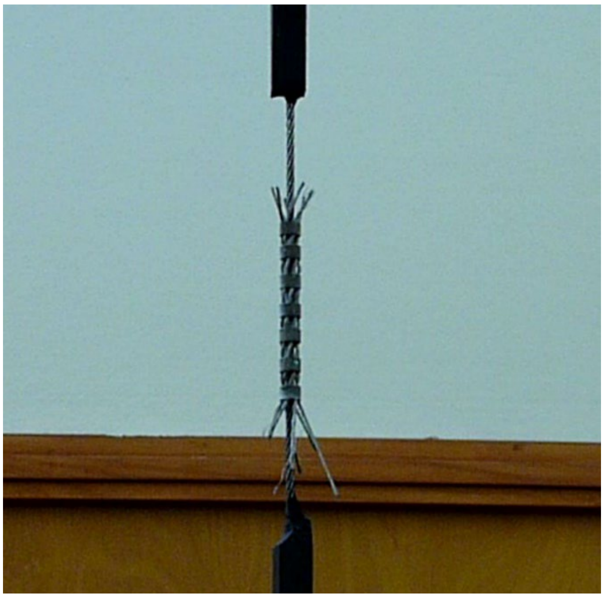

t = 0s

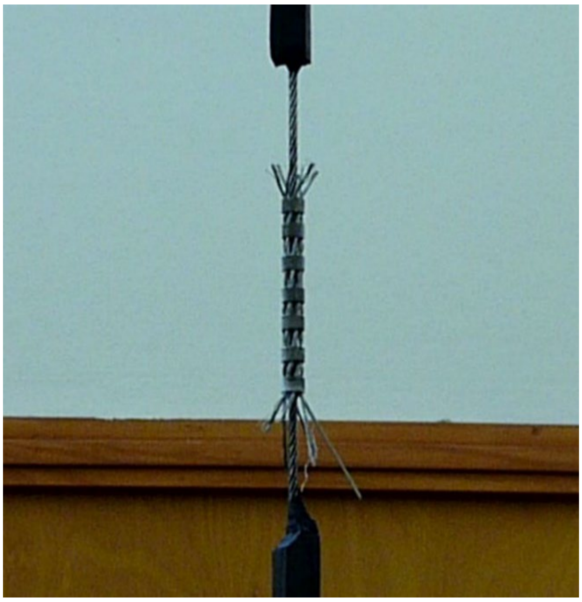

t = 24s

t = 48s

t = 72s

Figure 7.6 Testing and failure sequence (t = 0–72 seconds) for seven-ferrule connector wire and steel wire rope with same direction of rotation

The results shown in Figure 7.7 show test results of a seven-ferrule splice assembly. Connector wires and steel wire rope pitch have opposing directions of rotation.

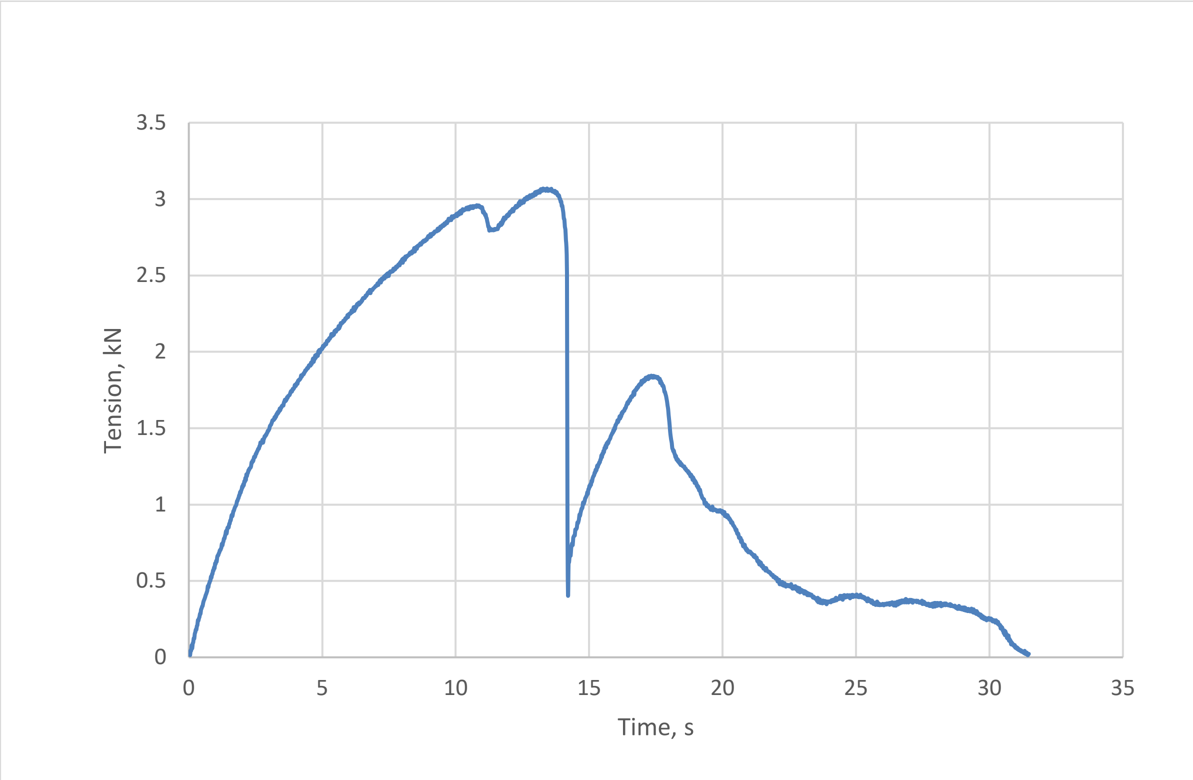

Figure 7.7 Splice assembly, seven-ferrule connector wire and SWR with opposing directions of rotation

By having the connector wires in the opposite direction of rotation, the assembly was able to resist torsion more effectively. The video analysis shows the outer connector wire maintaining its pitch while under increasing strain for a given period. This resistance to torsion allowed the assembly to resist over 3 kN Failure only occurred when the connector wires could oppose the resistance and began to slip through the ferrule guide holes. The slipping of the connector wires through the ferrule can be seen after 13 seconds. After approximately 15 seconds, friction between ferrule and ferrule connector wire builds, allowing the assembly to reach nearly 2 kN before failing again. The mode of failure in this case was wire slipping through ferrule guide holes. Inspection of assembly after testing revealed no obvious ferrule damage or sheared thread.

The sequence shown in Figure 7.8 is for a seven-ferrule assembly; connector wire and steel wire opposing rope have opposing directions of rotation.

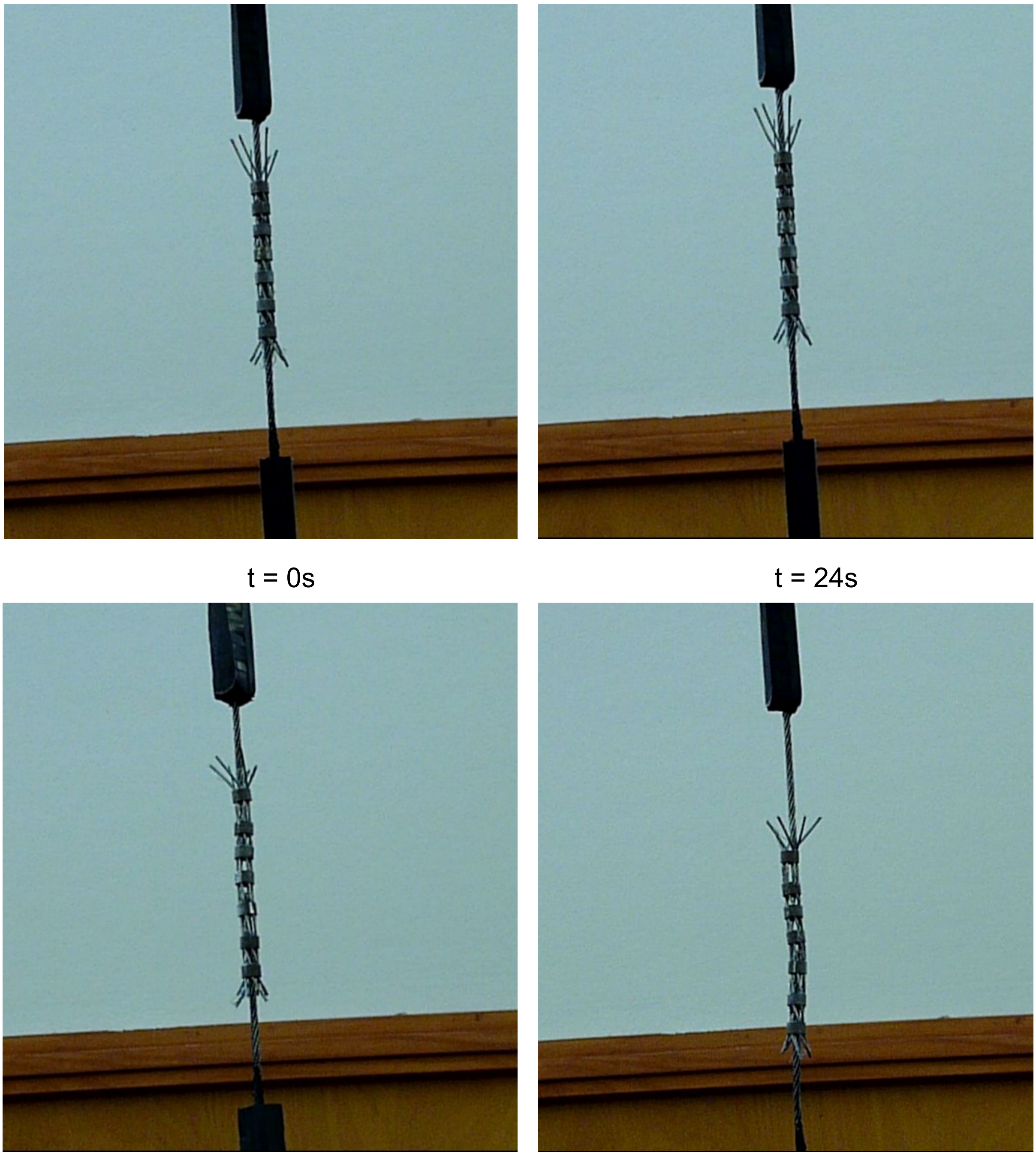

t = 0s

t = 24s

t = 48s

t = 96s

Figure 7.8 Testing and failure sequence (t = 0–96s) for seven-ferrule connector wire and steel wire rope with opposing directions of rotation

Figure 7.9 shows test results of a nine-ferrule splice assembly; connector wires and steel wire rope pitch share the same direction of rotation.

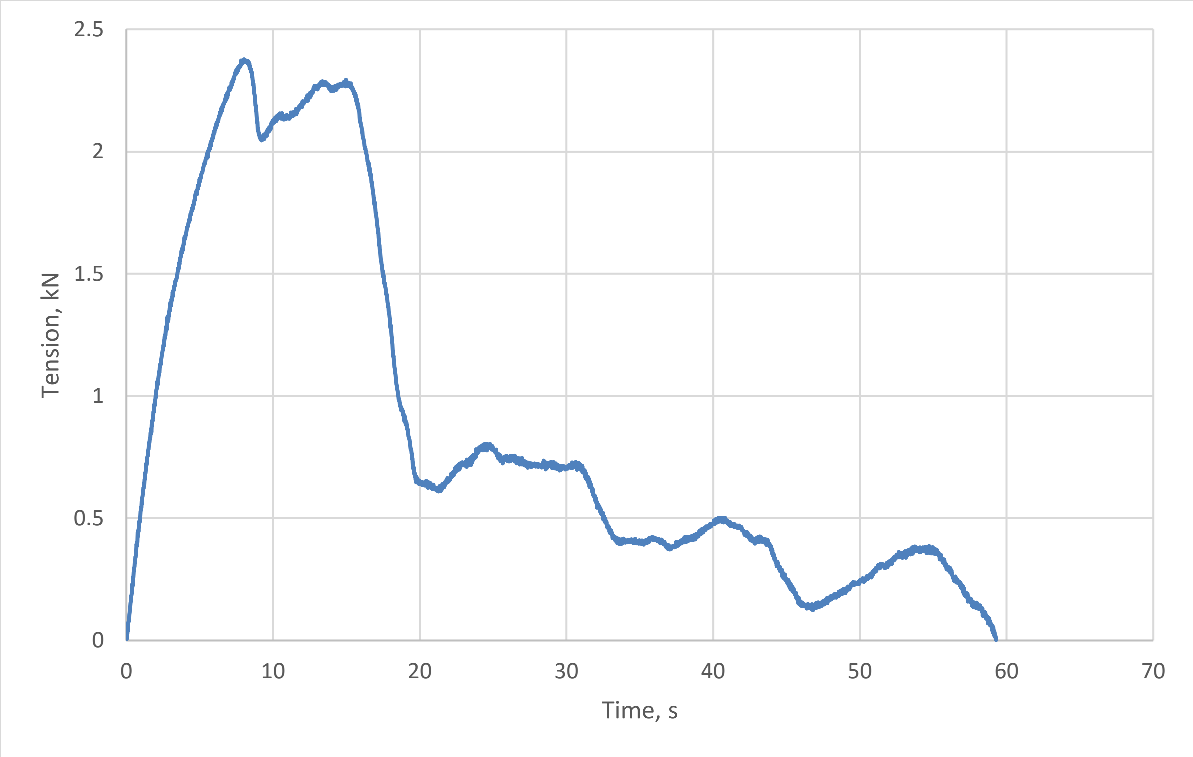

Figure 7.9 Splice assembly, nine-ferrule connector wire and SWR with inline direction of rotation

Like the seven-ferrule assembly, maximum tension is achieved quickly, until the adhesive fails to resist torsion and begins to unwind. The increase from seven to nine ferrules meant that there was more bonded surface area to resist torsion, thereby increasing the assembly's peak load capacity. With a significant increase in ferrule numbers, it may be possible to achieve the maximum required load capacity; however, this would mean that only the adhesive would be resisting torsion and there would be no utilisation of mechanical advantage (i.e., opposing connector wires resisting torsion).

The sequence shown in Figure 7.10 is for a nine-ferrule assembly; connector wire and steel wire with same direction of rotation.

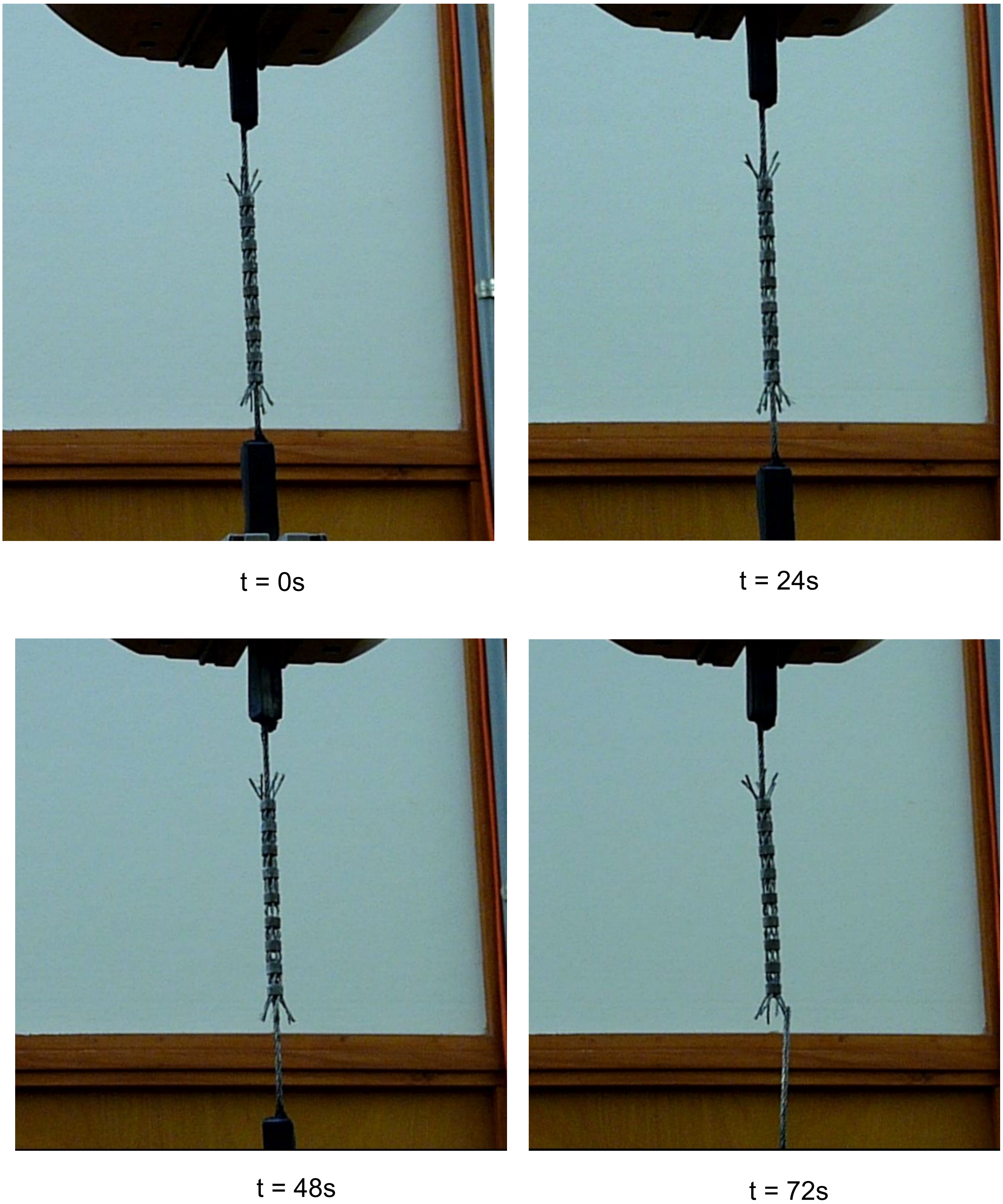

Figure 7.10 Testing and failure sequence (t = 0–72s) for nine-ferrule assembly, connector wire and SWR with same direction of rotation

Figure 7.11 below shows test results of a nine-ferrule splice assembly. Connector wires and steel wire rope pitch have opposing directions of rotation.

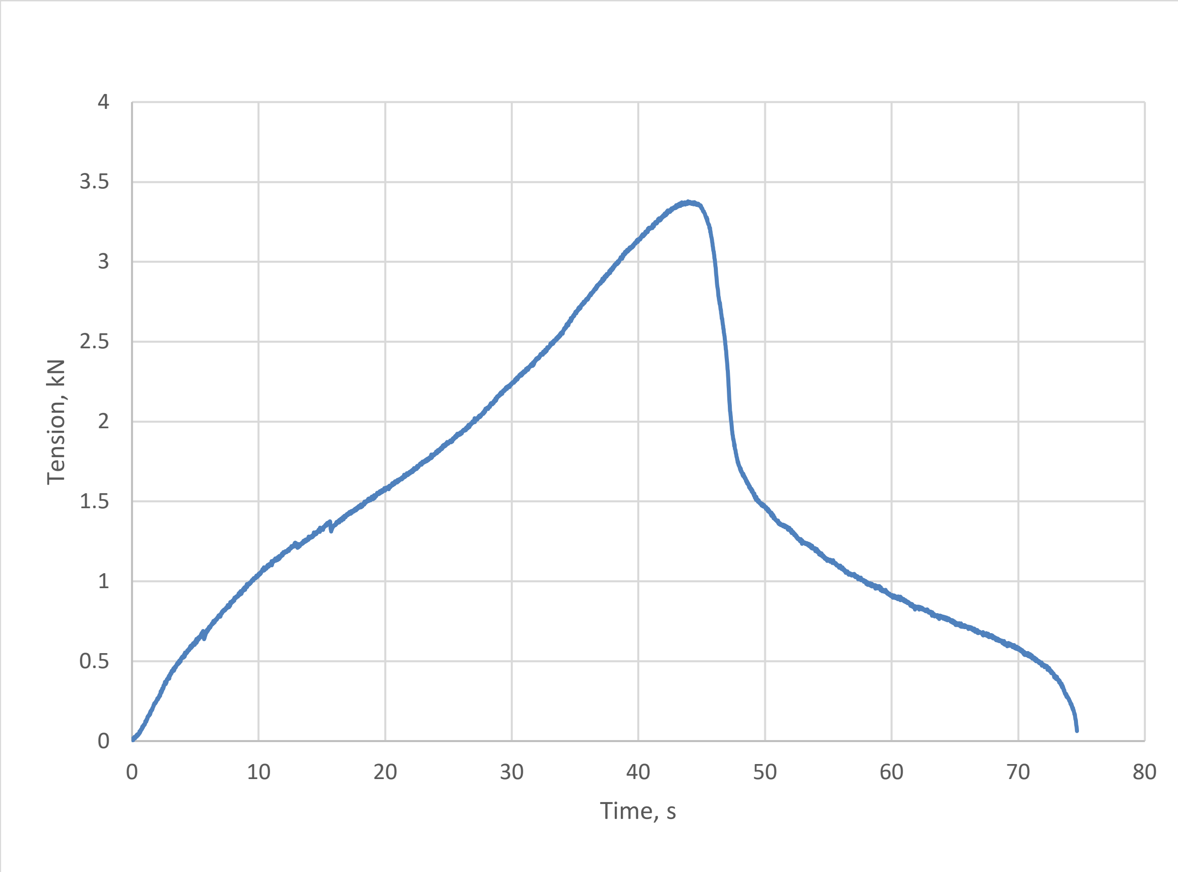

Figure 7.11 Splice assembly, nine-ferrule connector wire and SWR with opposing directions of rotation

Again, the time required to reach its maximum load capacity of 3.4 kN is longer than when ferrules are in-line. Again, it opposes rotation using adhesive bonding and mechanical advantage to counter the steel wire ropes' natural tendencies to rotate while under tension. Once the load through the steel wire rope is too great, it begins to straighten the connector wires, adding slack to the system. At this point, the assembly will begin to fail by unwinding from the steel wire rope and releasing completely.

The sequence shown in Figure 7.12 is for a nine-ferrule assembly. Connector wire and steel wire opposing rope have opposing directions of rotation.

t = 36s

t = 60s

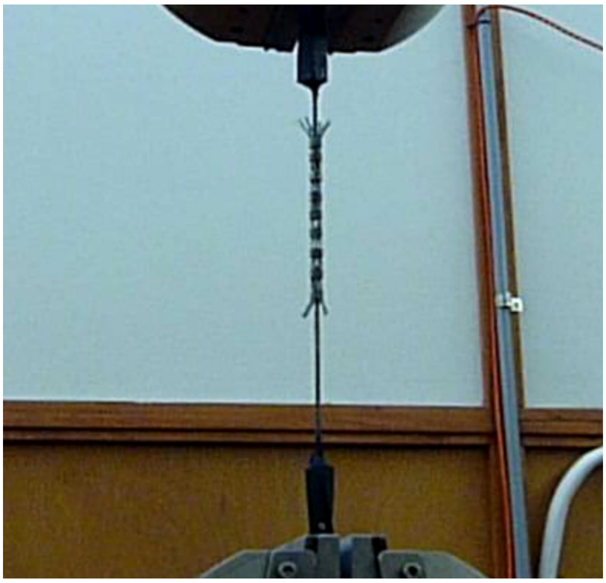

t = 84s

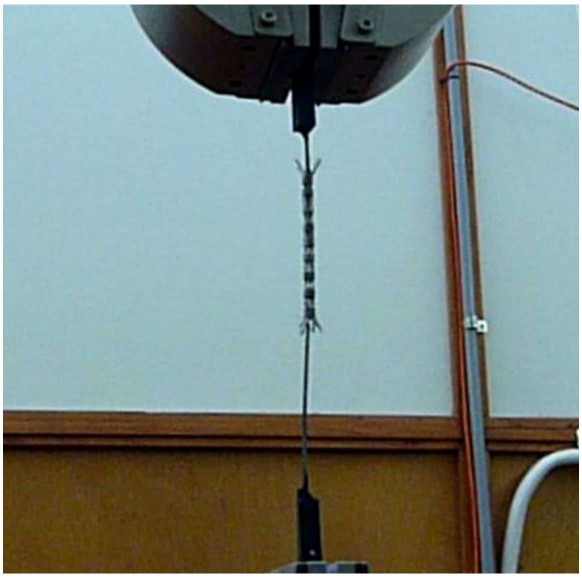

t = 108s

Figure 7.12 Testing and failure sequence (t = 36–108s) for nine-ferrule connector wire and steel wire rope with opposing directions of rotation

Figure 7.13 shows test results of an 11-ferrule splice assembly. Connector wires and steel wire rope pitch share the same direction of rotation.

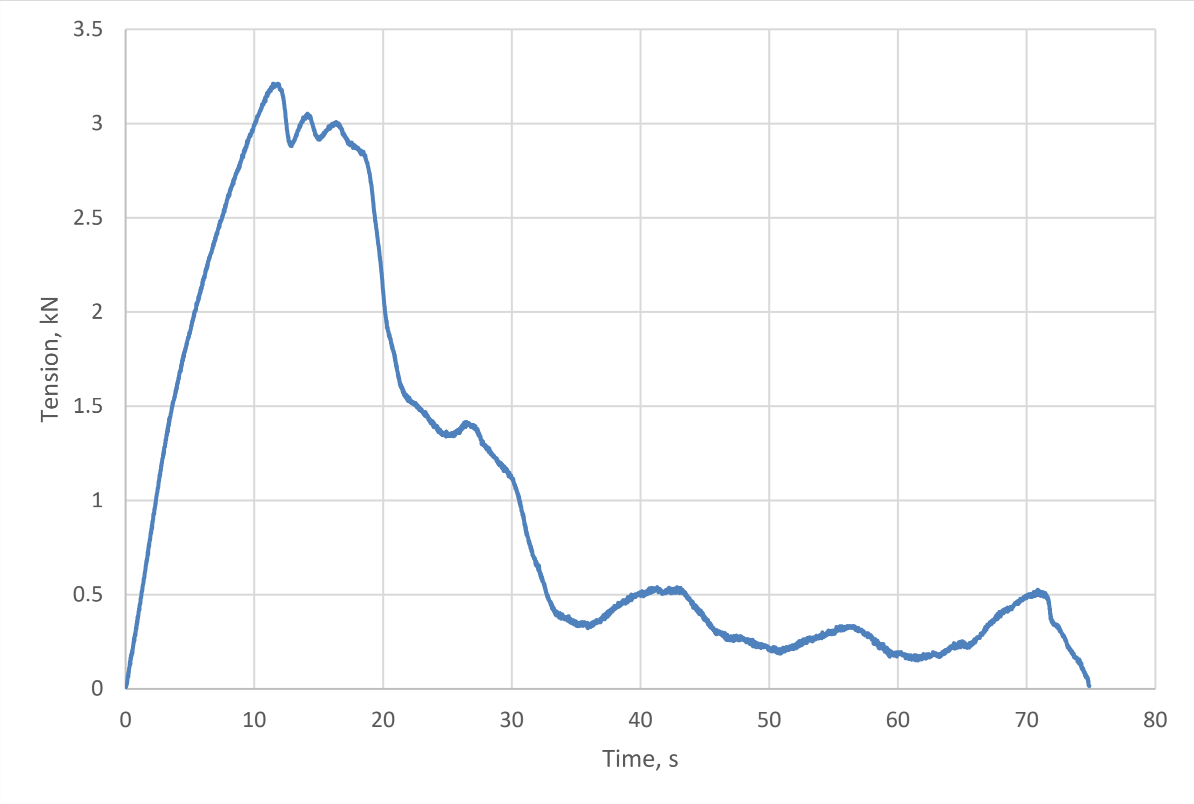

Figure 7.13 Splice assembly, 11-ferrule connector wire and SWR with inline direction of rotation

The model begins build load quickly, eventually reaching just over 3 kN before beginning to unwind and lose tension. Like all the other inline systems, the only thing resisting rotation is cyanaocrylic adhesive bonds between components. The assembly can resist more torsion due to the increase number of ferrules; however, it eventually fails when the adhesive bond fails, allowing the assembly to unwind from the steel wire rope. The assembly has not failed because of exceeding its maximum yield; it has failed because the adhesive has sheared.

The sequence shown in Figure 7.14 is for an 11-ferrule assembly. Connector wires and steel wires have the same direction of rotation.

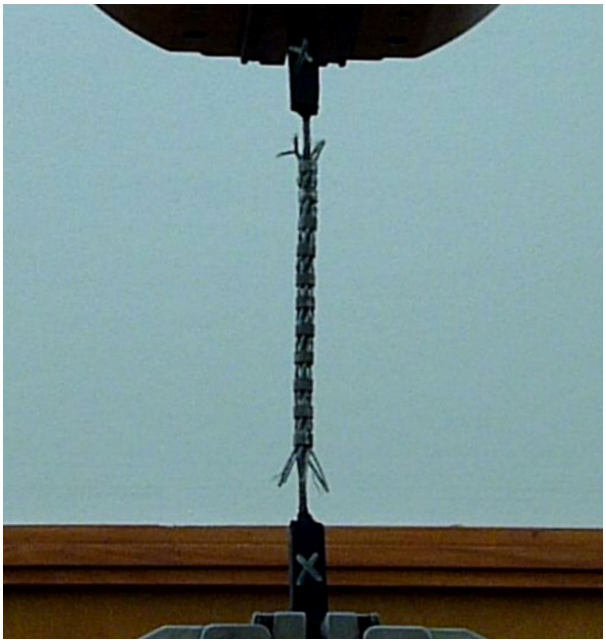

t = 36s

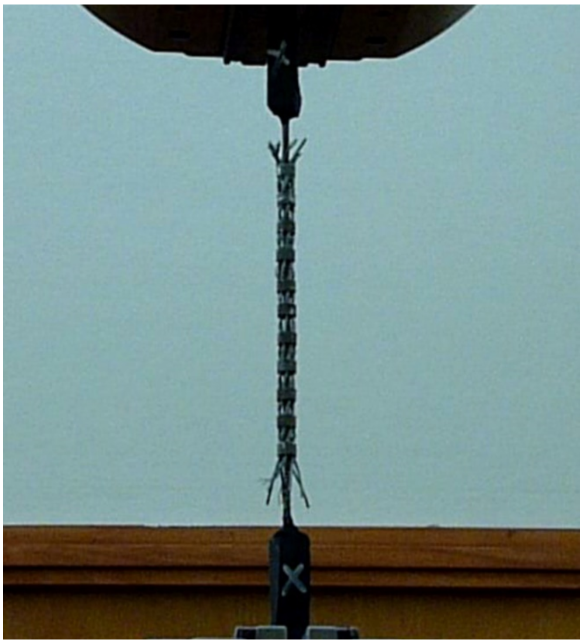

t = 72s

t = 84s

t = 108s

Figure 7.14 Testing and failure sequence (t = 0–72s) for 11-ferrule assembly, connector wire and SWR with same direction of rotation

Figure 7.15 show test results of an 11-ferrule splice assembly. Connector wires and steel wire rope pitch have opposing directions of rotation.

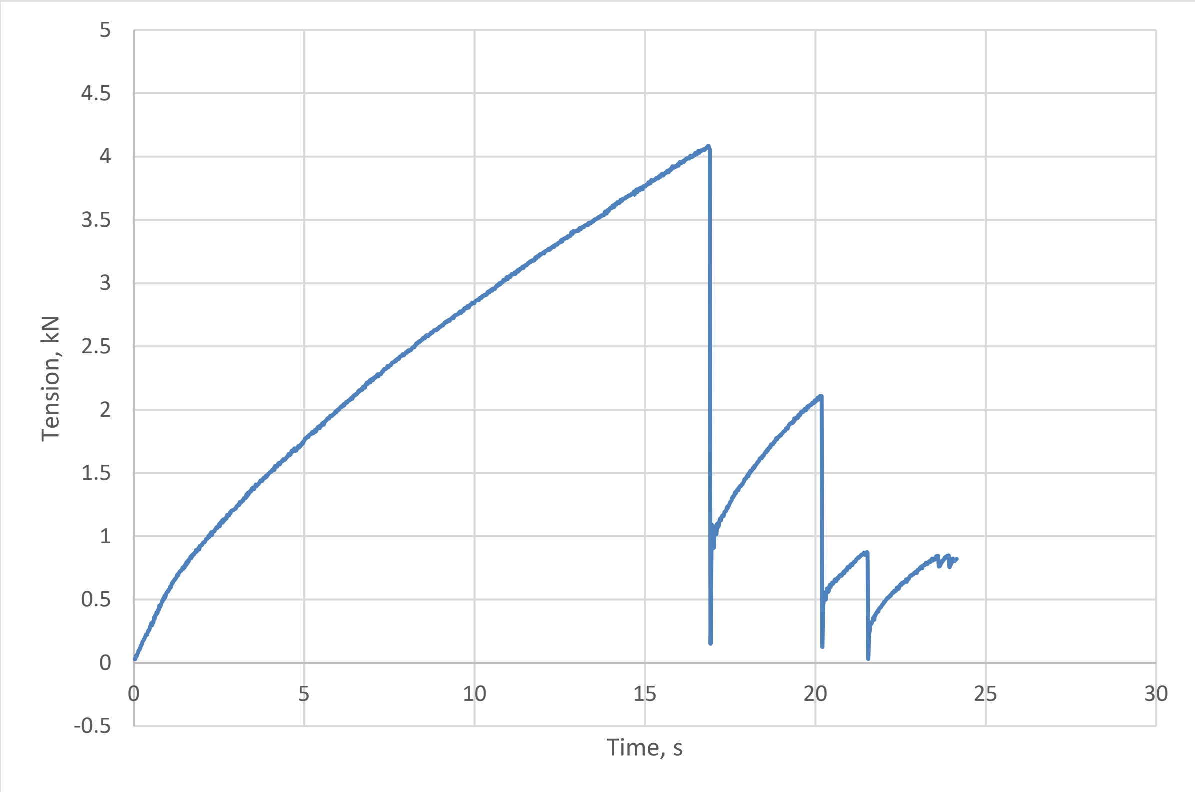

Figure 7.15 Splice assembly, 11-ferrule connector wire and SWR with opposing directions of rotation

The 11-ferrule splice was able to reach a maximum load capacity of just over 4.0 kN by increasing the number of ferrules from nine to 11, the assembly had sufficient bonding surface area and mechanical advantage to resistant steel wire rope torsion while under tension. Failure mode of this splice assembly was due to rupture of connector wires holding the ferrules together and not an eventual unwinding of ferrules, which has been the failure mode for five of the six tests. The assemblies tested were predicted to fail at 3.6 kN as this is the maximum total load capacity of the connector wires. For the assembly to achieve an 8.4 kN load rating, high-tensile wire, additional wires or a combination of both will have to be used.

The sequence shown in Figure 7.16 is for an 11-ferrule assembly. Connector wires and steel wires opposing rope have opposing directions of rotation.

t = 0s

t = 60s

t = 120s

t = 120s

Figure 7.16 Testing and failure sequence (t = 0–180s) for 11-ferrule connector wire and SWR with opposing directions of rotation

7.2 Result Summary

Figure 7.17 is a summary of peak loads for inline and opposing ferrule assemblies.

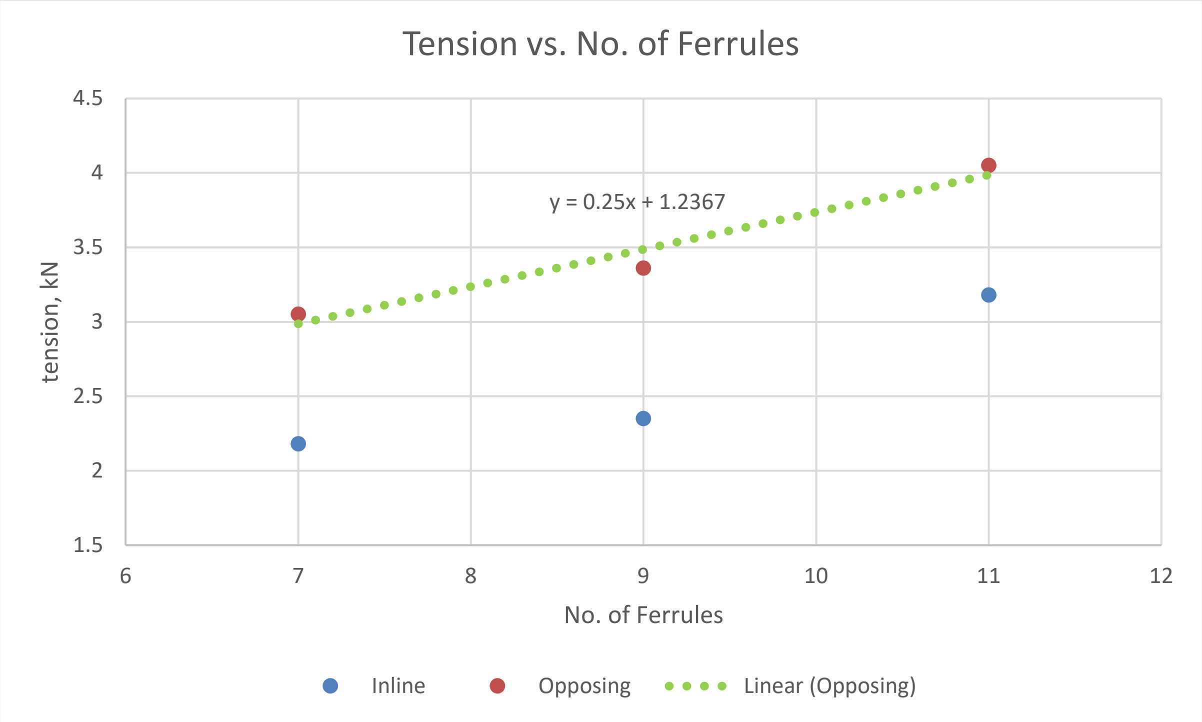

Figure 7.17 Load failure summary based on number of ferrules for both online and opposing assembly design

The figure clearly shows that ferrule connector wires with opposing directions of rotation can achieve a significantly high peak load rating. Based on observation of tensile testing, higher loads can be achieved because both adhesive strength and mechanical advantage are used to resist steel wire rope torsion. Because of the limited number of assemblies tested, it is difficult to predict accurately how many ferrules are required to achieve the load rating for the 2.8 mm diameter steel rope commonly used in ST630 conveyor belts.

If the assumption was made that all components used to make up a splice assembly would not fail under yield, Figure 7.17 could cautiously predict the number of ferrules required to achieve a required load rating. Based on an approximate gradient of 0.25 kN/ferrule, an additional 21 ferrules would be required to reach an 8.4 kN breaking load capacity, as per AS1333. With 5 mm spacings, this would produce a splice assembly that is only 300 mm in length; still significantly smaller than traditional splices.

With further investigation, it may be possible to further reduce the number of ferrules required, by investigating different adhesives and assessing the effects of using either liquid polyurethanes or vulcanised rubber to encase the assembly after construction. Both materials have a unique spring-dampening system, which could also help resist assembly torsion. This testing would be additional and outside the scope of this work.

Care was taken to construct each assembly; however, it should be noted that each assembly was constructed in a non-controlled environment, with varying temperatures and humidity, among others. These two variables are critical when using adhesive as they can affect curing times and overall bonding strength. Finally, any future test sample should be constructed in a laboratory environment to ensure greater confidence in results.

8 COMMERCIAL AND SAFETY IMPACT

8.1 Commercial

In December 2017, the spot price for 62% CFR iron ore was USD71.83/tonne [25]. Some Australian port facilities, including Parker Point and East Intercourse Island, can load ships at a throughput of 10,000–14,000 tonnes per hour. This equates to approximately USD718,300–USD1,005,620 per hour in lost time production every time a conveyor is inoperable. By improving conveyor belt splice design and reducing construction time, it is possible to increase production and profits without upgrading existing infrastructure. With some steel cord belts taking 12 or more hours to construct, reducing this time by even 10% could translate into millions of dollars in additional production.

8.2 Safety

A poorly constructed belt splice can lead to catastrophic failure, leading to significant downtime, equipment damage and potentially injury or loss of human life. Bulk material transported by the conveyor can spill on to walkways or overpasses, crushing and suffocating any person unfortunate to be in proximity. Many technologies, along with safety checks and inspections, exist. A conference paper on a novel non-destructive test for belt splice by James demonstrates a practical method of determining the strength of a steel cord belt splice constructed in the field [13]. When constructing a steel cord belt splice, an edge bar sample can be produced in parallel (see Figure 8.1 and Figure 8.2).

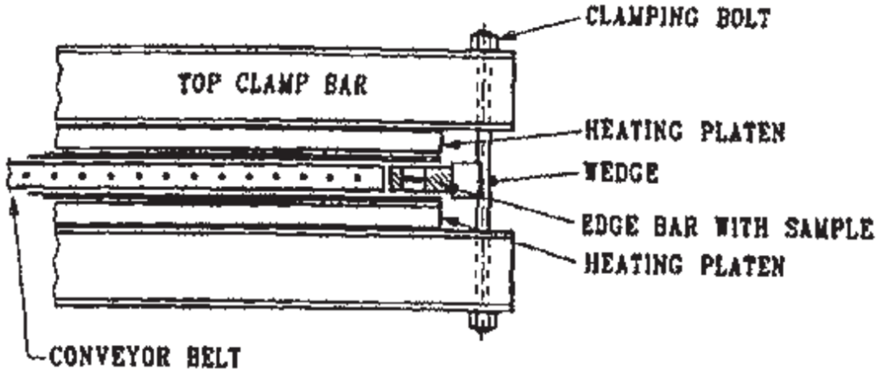

Figure 8.1 Edge bar sample while vulcanising steel cord belt splice [13]

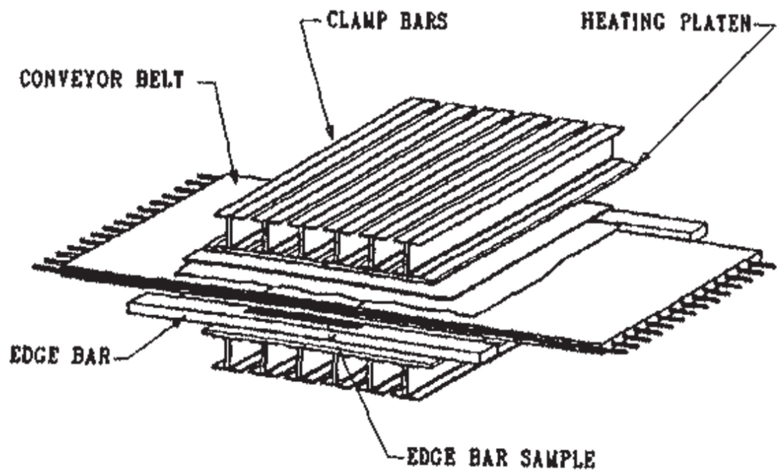

Figure 8.2 Section of edge of belt [13]

This is an effective method of testing the strength of a splice as it replicates site conditions; however, results are not in real time, and not available until a rubber pull-out test can be completed at an offsite facility. Meanwhile, the conveyor will operate untested, with splice strength unknown. If test results indicate a flawed splice, the conveyor would cease operations and a new splice would be constructed. Industry experience suggests that these tests are seldom completed; additionally, since they do not give real-time results, there is a possibility that a splice failure could occur prior to obtaining results.

Conveyor belt manufacturers and researchers have for many years investigated online conditioning monitoring to detect cord and splice defects. These include simple methods such as visual inspection, the grid line method, which involves marking the splice, bulge detection mechanisms and even x-ray machines. Though these methods can be effective, they are difficult to apply and generally involve slowing the belt down or stopping it all together. A method investigated by Barfoot explores how the displacement of steel cords relative to those adjacent can create variations in a magnetic field [3]. This displacement can signify poor adhesion within a splice and could be a potential point of failure. Figure 8.3 and Figure 8.4 illustrate the schematic sensor arrangement and magnetic field used to detect cord movement.

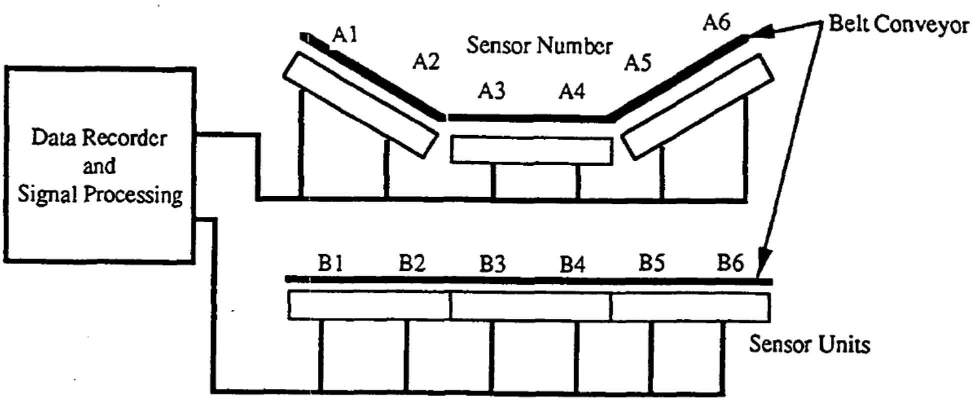

Figure 8.3 Sensor arrangement for magnetic field detection [3]

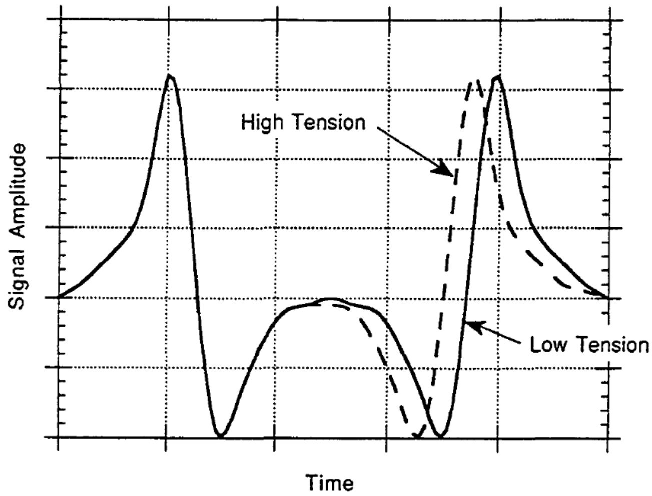

Figure 8.4 Difference between splice signals taken at high and low tension [3]

The variation between the high- and low-tension signals is used to help determine cord movement.

There are many systems and processes that can be used to detect issues with steel cord belt splices; however, because of cost, poor training, time constraints and environment, these tools are typically not used. The reality is that there are many conveyor belts in the world not subject to a high level of monitoring. As automation increases, this type of technology will be common; however, until then, belt splices will continue to be a financial and safety liability.

9 CONCLUSION

The development of stronger, more durable fabric and steel cord conveyor belts has helped designers and engineers construct conveyors capable of travelling long distance over undulating terrain. With the development of longer and high-tension conveyors steel cord and fabric belts have increased in strength with some conveyor belts now exceeding a design strength of 10,000kN/m. As these tensions continue to increase, the method in which conveyor belts are joined together become more and more critical. Advancements in splice technology have improved construction with Goodyears' development of preformed splice covers for steel cord belts and Conti adhesive based cold bonding systems to join fabric belts. Conveyor belt splices are extensively tested to ensure their strength and fatigue limits. Both environmental and constructability impacts are also incorporated into belt safety factors which takes a level of unknown into consideration.

Regardless of these improvements and inclusion of safety factors, conveyor belt splices continue to fail causing millions of dollars each year in unscheduled downtime and exposing workers and personnel to potential injury. If a splice is constructed as per manufacturer requirements, the conveyor system is design correctly, properly operated and maintained then a belt splice should not fail prematurely Unfortunately, the combination of financial pressures along with sometimes unskilled labour ensure belt splice failures are an ongoing issue on site.

One method of reducing the occurrence of belt splice failures is by simplifying belt splices and reducing construction time. Not only would this improve lost time production, it would lessen the introduction of constructability error. Though both fabric and steel cord splices are of concern, focus has mainly been placed on addressing and simplifying steel cord splice construction.

This study has developed a novel method of splicing individual steel cords to allow continuity within the belt. This removes the reliance on using vulcanised rubber as a bonding method and its requirement to sustain belt tensions through shear. Laboratory testing using the MTS tensile test machine has demonstrated that a 2.8mm diameter steel cord used in the construction of a ST630 conveyor belt can be joined and sustain load exceed 4kN before failing using a proposed splice assembly prototype.

Preliminary FEA confirms that current material used, and design of ferrules will need to improve if it is to be used under increased loads with the 316SS steel used to be replaced with a higher yield material such as titanium. This material would be a suitable candidate as can also be 3D printed in mass. There is much benefit to this as complicated manufacturing techniques would be need if manufactured through casting, drilling and machining.

By improving the materials used and optimising the design with the use of additional ferrules, the proposed splice assembly could be used to potentially improve efficiency and safety within the conveyor belt industry.

10 FURTHER DEVELOPMENT

The proposed splice assembly concept is a novel method to join steel wire rope effectively and safely; however, it is still in its infancy and further development is required. The following is a summary of considerations to further develop the concept.

10.1 Static and Dynamic Testing

Additional splice assemblies still need to be tested in the MTS tensile testing machine. The number of ferrules will need to be increased until the required static tensile loads can be achieved. In addition to this, each assembly should be fully encased in either vulcanised rubber or, alternatively, a quick-drying liquid polymer. By doing so, it should be possible to determine how much additional torsional resistance this applies when the assembly is under tension. If static testing is successful, a full belt splice would be constructed. The splice can then be placed in a dynamic testing rig, where its dynamic fatigue strength (according to DIN22110-3 [26]) can be determined. Figure 10.1 is the dynamic test rig in Hannover, Germany and used by belt manufactures from all around the world for testing.

Figure 10.1 300 kN/revolution dynamic fatigue strength test rig, Hannover Germany [27]

10.2 Material Selection and Component Testing

Each component that makes the assembly needs to be tested individually to determine its characteristics and suitability for this application. Initial parts were based on accessibility of materials and ease of construction. Ferrules were metal 3D printed in a powdered form of stainless steel with a yield strength of approximately 500 MPa. It is likely that stress on these ferrules will exceed this; therefore, high-yielding materials such as titanium will need to be considered. Steel wire rope used in the ferrule connector was also low yielding, as it was made from marine grade 316SS. Future testing will require the use of high-tensile steel wire to achieve the required splice assembly working requirements.

10.3 Construction and Tensile Testing

Because of the complexity involved in the construction of each splice assembly concept, only six were successfully created. To increase confidence in the design, additional assemblies should be tested in a tensile test machine. Further, multiple assemblies encased in both vulcanised rubber and polyurethane should be tested to determine their effects in terms of resisting torsion.

10.4 Further Testing Samples

In order to validate the ferrule assembly concept, additional tensile testing is required. By constructing a larger sample base of ferrule assembles at different diameters, stability and consistency in results could be achieved. Table 10.1 below shows number required.

Table 10.1 Total number of ferrule assemblies required for tensile testing

Testing Lot	No. of ferrules	Assemblies 8mm dia.	assemblies 10mm dia.	assemblies 12mm dia.	Assemblies 14mm dia.
1	5	5	5	5	5
2	7	5	5	5	5
3	9	5	5	5	5
4	11	5	5	5	5
5	13	5	5	5	5
6	15	5	5	5	5
Total	**-**	**30**	**30**	**30**	**30**

As a minimum, one hundred and twenty ferrule assemblies would be needed for a good sample group. After some practice, it could be possible to make up to four assemblies per day however, this would still take one to two months of work to complete.

At this point making components this small still take significant time, further research will be required to create an automated process. Tooling will also need to be designed and prototyped.

At this stage of the work, splice ferrule assemblies have only been tested using a static tensile testing rig. Once the static testing verifies the concept, dynamic testing will be required to simulate the cyclic loading that occurs during normal conveyor operations.

Reference

[1] P. Commins, "How the iron ore price busted above $US100 a tonne," in *Financial Reveiw*, ed: Financial Review, 2019.

[2] G. Barfoot, "Condition Monitoring of Steel Cord Belt Conveyor Splices," presented at the 1993 National Conference on Bulk Materials Handling: Preprints, 1993.

[3] Phoenix, Phoenix Conveyor Belts Design Fundamentals, Hamburg Germany: Phoenix, 2004, p. 64. [Online]. Available.

[4] C. W. a. A. Roberts, "Continuous Conveyors," 2018.

[5] Bridgestone, "Vulcanized Splicing For Steel Cord Conveyor Belts, One-Step Method, Two-Step Method," Unknown.

[6] O. W. E. Dr-Ing Rainer Alles, Prof. Dr.-Ing. W.S.W Lubrich, Dip-Ing G. Bottcher, Dip-Ing H. Simonsen, Dip-Ing. H. Zintarra, *Contitech Conveyor Belt System Design*. Contitech Transportbandsysteme GmbH D-30001 Hannover 1994.

[7] "All-State Belting," S. C. B. Splicing, Ed., ed: All-State Belting, 2014.

[8] P. S. M Otrebski, "Gemetrical and mechanical properties of steelcord belt splices," presented at the Beltcon 6, 1991.

[9] W. S. Weigang Song, Xiaosen Li, "Finite Element Analysis of Steel Cord Conveyor Belt Splice," S. Northeastern University, China, Ed., FEA ed. IET , London 2009, p. 6.

[10] P. E. Rengifo, "New Splice Assembly Technique For Wire Reinforced Belting " *Bulk Solids Handling,* vol. 24, no. 1, 2004.

[11] A. Harrison, "Limitations of theoretical splice design for steel cord belts," (in English), *Bulk Solids Handling,* Article vol. 14, no. 1, pp. 39-43, 01 / 01 / 1994.

[12] I. Pearson and M. Pickering, "The determination of a highly elastic adhesive's material properties and their representation in finite element analysis," *Finite elements in analysis and design,* vol. 37, no. 3, pp. 221-232, 2001.

[13] G. James, "A Non-destructive Test for Belt Splices, How Good are you Splices," presented at the Bulk Solids Handling, Clausthal- Zellerfeld, Germany, 1992.

[14] N. Lavoie, "Innovations in Hybrid Structural Instant Adhesive Technologies," Society of Plastics Engineers, 2015.

[15] N. Lavoie, "Time is money: High speed adhesive solutions for instant bonding," 2016.

[16] Henkel, "Loctite 4090 Technical Datasheet," ed: Henkel, 2013.

[17] C. Czaderski, E. Martinelli, J. Michels, and M. Motavalli, "Effect of curing conditions on strength development in an epoxy resin for structural strengthening," *Composites Part B: Engineering,* vol. 43, no. 2, pp. 398-410, 3// 2012.

[18] G. Kastratović, N. Vidanović, V. Bakić, and B. Rašuo, "On finite element analysis of sling wire rope subjected to axial loading," *Ocean Engineering,* vol. 88, pp. 480-487, 2014/09/15/ 2014.

[19] S. Cabrera, "MTS Tensile Test Machine," 20180119_132125.jpg, Ed., ed. University of Newcastle: Sergio Cabrera, 2018.

[20] S. Cabrera, "ST630 Belt Pull-Out Samples ", 20180119_112027.jpg, Ed., ed. University of Newcastle: Sergio Cabrera, 2018.

[21] *Conveyor Belting of Elastomeric and Steel Cord Construction*, 1994.

[22] D. U. Wenzheng, M. A. Baozhu, X. I. E. Zheng, C. A. O. Dazhi, and W. U. Peng, "Finite element analysis on the wire breaking rule of 1x7IWS steel wire rope," *MATEC Web of Conferences,* Article vol. 108, pp. 1-5, 06// 2017.

[23] S. P. Ltd, *Strand 7 reference Manual* (no. 2.4). Sydney, NSW: Strand 7 Pty Ltd, 2015.

[24] "<AS1333-1994.pdf>."

[25] (2018, 7 May 2018). *Market Index*. Available: https://www.marketindex.com.au/iron-ore

[26] *DIN 22110-3 : 2015, Testing methods for conveyor belt joints - PART 3: Determination of strength for conveyor belt joints (Dynamic Testng Method)*, 2015.

[27] "300kN Hannover Test Rig," vol. 1.88MB, k. H. T. Rig, Ed., ed. Hannover Germany, 2018.

APPENDICES

Appendix A – Operators Splice Manual

Appendix B – Finite Element Model Construction

Appendix A

Operators Splicing Manual

1. CONTENTS

2. INTRODUCTION

The following demonstrates the process required for splice steel cord belts using the ferrule connector assemblies.

3. STEP 1 PREPARE WORK SITE

Before splicing can commence, both belt ends must be securely clamped and laying on a belt splicing table completely covered by a positively pressurised tent. This will ensure the splice itself is free from air born particles and moisture.

4. STEP 2 PREPARE BELT SPLICE

Steel cord belt splice preparation will depend on the belt rating. This is to ensure that when the splice is completed. The pitch to diameter ratio is as per manufacturers requirements. This ratio is achieved by splicing in steps. i.e. 1-step, 2-step etc.

The process for preparing the splice i.e. removing covers and stripping rubber off cords etc. is documented by all belt manufacturers. A good practical methodology can be found in Nilos 'Instructions for Splice Steel Cords'.[1] Once prepared, the belt splice is ready for joining.

5. STEP 3 CONNECT STEEL CORDS

Once all cords are exposed, the belt must be sufficiently stripped of remaining rubber so that ferrule connectors can screw on the steel wire rope as shown below in Figure 5.1.

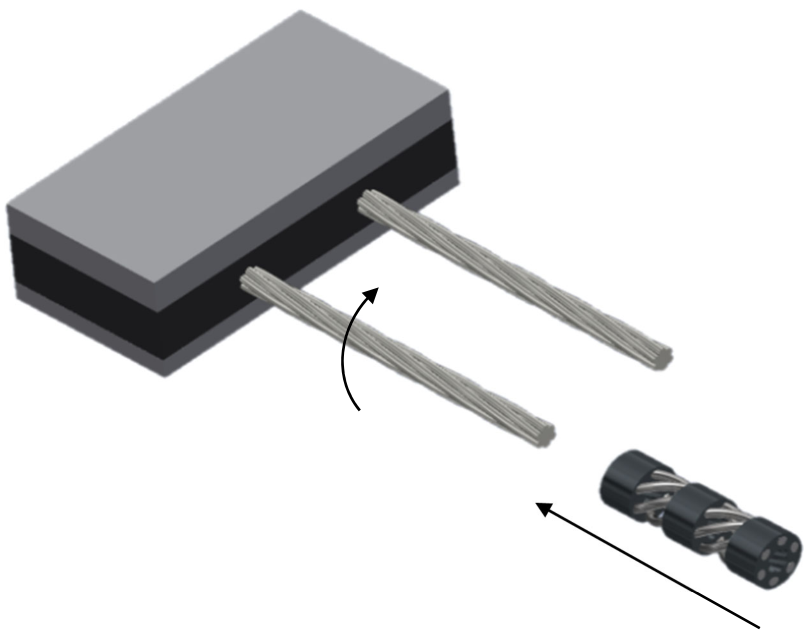

Figure 5.1 Screwing ferrule on to belt steel wire rope

The ferrule is then back screwed on to the opposing wire as shown in Figure 5.2

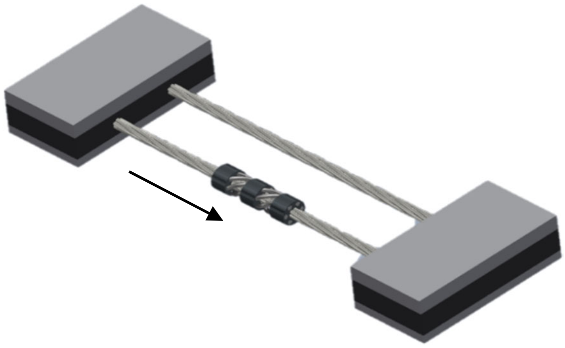

Figure 5.2 Joining opposing steel cords by screwing ferrule assembly to cords.

Adhesive is then squeezed through the ferrule pilot hole to prevent the ferrule unwinding off the steel cord before splice can be vulcanised as illustrated in Figure 5.3.

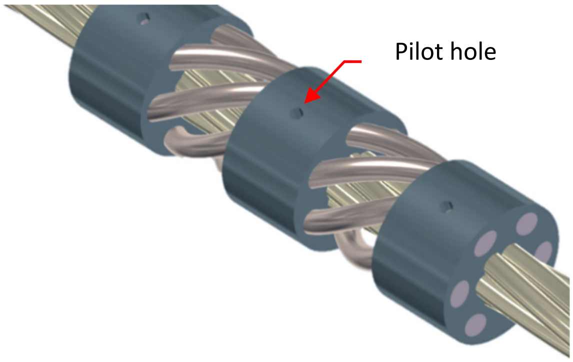

Figure 5.3 Adhesive pilot hole to fix ferrule assembly to cord.

6. SPLICE PREPARATION

Prior to preparing the splice for vulcanisation, the joint length of each cord must be measured. This is required to ensure that steel wire cords are evenly loaded. The splice is then built up of unvulcanised rubber noodles and covers as show in Figure 6.1

Figure 6.1 Splice construction with assembly ferrules

From here the splice methodology is the same as for any steel cord splice construction where the splice is pressed and heated until to pre-determined values allowing the rubber to seal and adhere to the steel wire ropes and ferrule assemblies. A typical vulcanising set looks that shown in Figure 6.2.

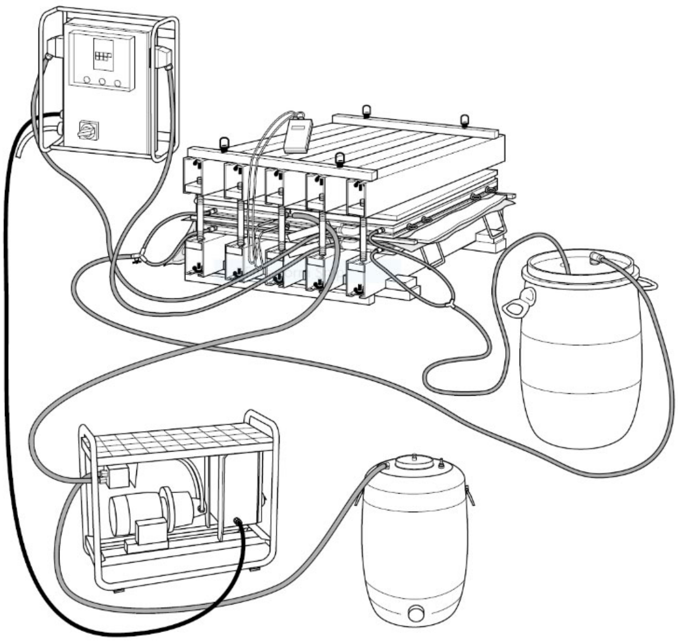

Figure 6.2 Typical vulcanising set up[1]

This typical set up can be used for splicing with ferrule assembly connectors without modification.

A Detailed method showing the full vulcanisation process can found in Nilos 'Instructions for Splice Steel Cords [1]

Reference

1. Nilos, *Instructiions for Splicing Steel Cord Belts* Nilos GmbH & Co. KG: Hilden, Germany. p. 22.

Appendix B

Finite Element Model Construction

CONTENTS

INTRODUCTION

The following is a brief summary of how the ferrule assembly model was created. This step by step process assumes that the reader has a reasonable background and understanding in finite element analysis.

Step 1 – Import CAD Model

A 3D model developed in Autodesk Inventor was imported into Strand as an Initial graphics exchange specification (IGES) file. This imported file type creates faces which can be further modified once in Strand 7 graphical user interface (GUI).

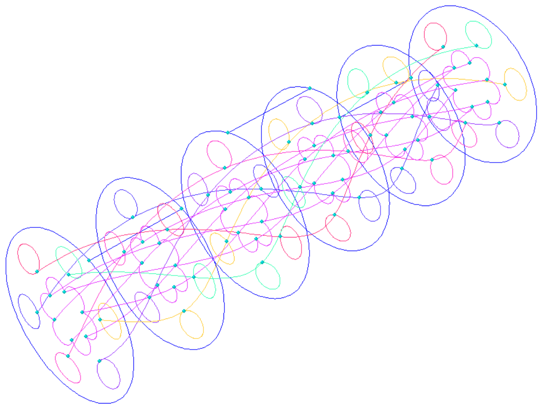

Figure 0.1 IGES geometry imported from Inventor into Strand 7

Step 2 – Clean and Prepare Model

The faces are then cleaned of unnecessary vertices and zipped together (if required) based on a set of default minimum tolerance. Due to the small size of the assembly parts, mesh density must be quite high. This is to improve aspect ratio as plates are not contorted as much around complex geometry. Correct aspect ratios are critical to shortening processing times and improving accuracy of results.

Before initial surface meshing, ferrule connector wires are separated from ferrules. This will allow beam element to be created later. These can be used to analyse interaction i.e. shear stress, displacement.

Below additional vertices are added to help find the centre point of each ferrule connector.

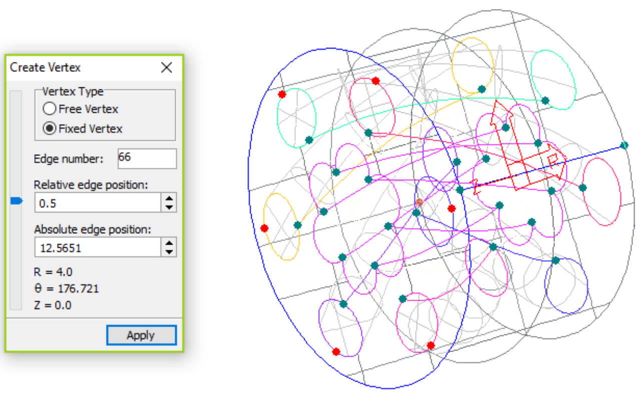

Figure 0.2 Adding additional vertex to assist with separating ferrule from ferrule connector wires.

A Universal Coordinate System (UCS) is created by selecting the outside as the reference

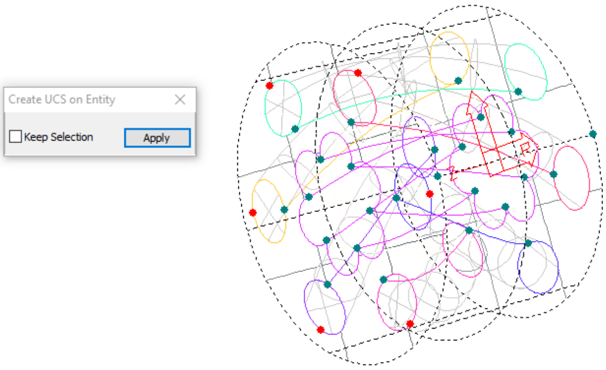

Figure 0.3 Selecting coordinate system to allow for extrusion along a helical path

Step 3 – Mesh Assembly

Surface is meshed (mesh will later be extruded to create brick elements). Surface meshed comprises of quad4 elements with a maximum 0.25mm edge length.

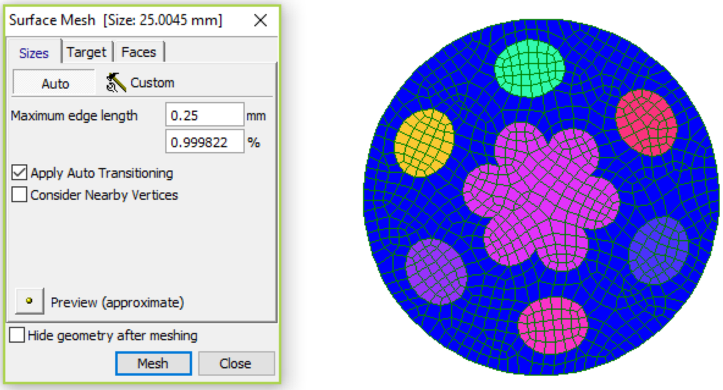

Figure 0.4 Ferrule surface meshing

Step 4 – Separating Assembly

The ferrule connectors are separated by detaching shared nodes then scaling the ferrule up to produce a small gap between parts

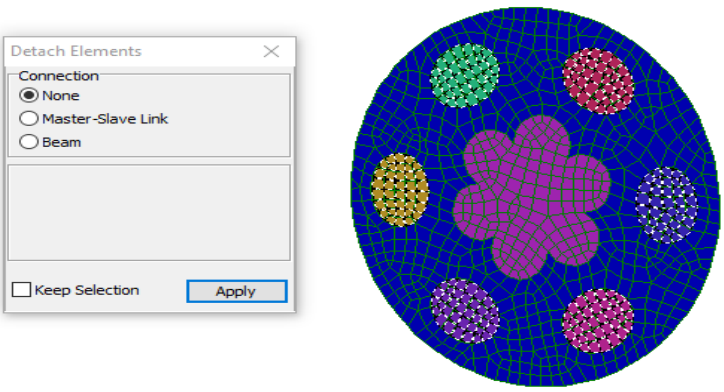

Figure 0.5 Ferrule Connector wires are selected

These are then hidden to allow for easier manipulation of ferrule surface.

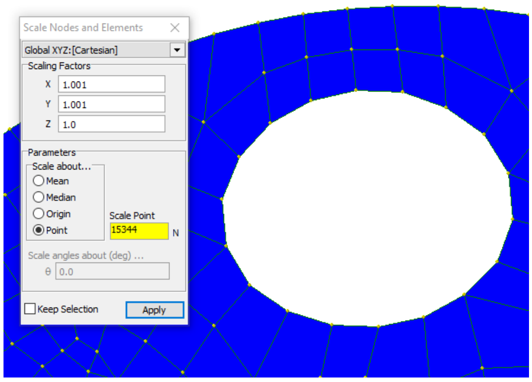

Figure 0.6 hole is increased by scaling 1.001 in x and y direction only

The creates a small gap between them as shown below,

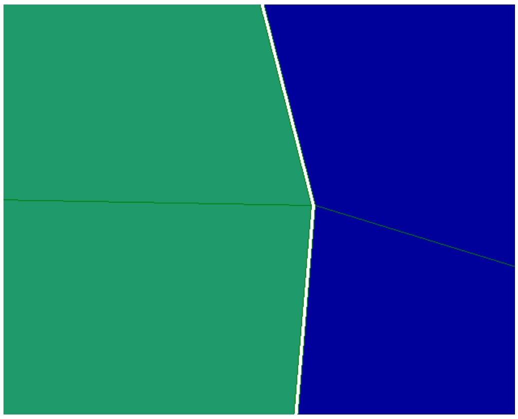

Figure 0.7 Gap created between ferrule and ferrule connector through scaling

Step 5 – Extruding

From here both steel wire rope and ferrule connectors are extruded using "Extrude by increment"

The path can be selected using "Set by points" i.e. use initial and final vertices to extrusion path.

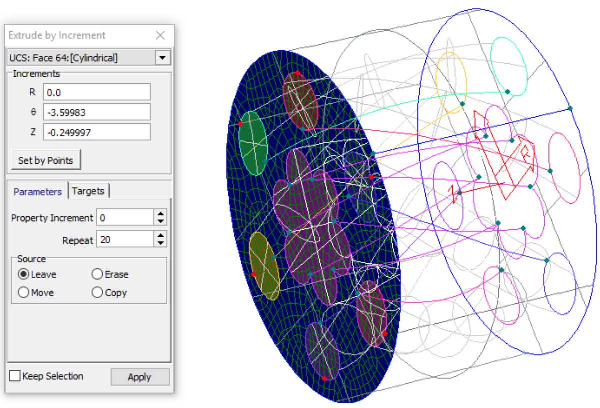

Figure 0.8

Will move forward with extrusion if **move** is selected in the **Source** option

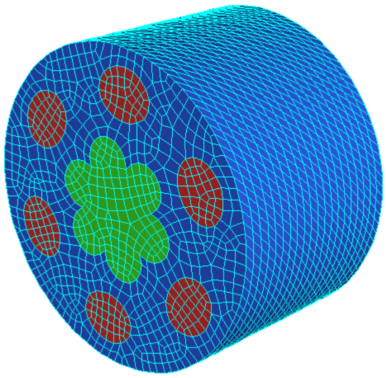

Figure 0.9 Ferrule Extruded from surface mesh

A single ferrule has now been developed, with further extrusion required to complete a multi ferrule assembly.

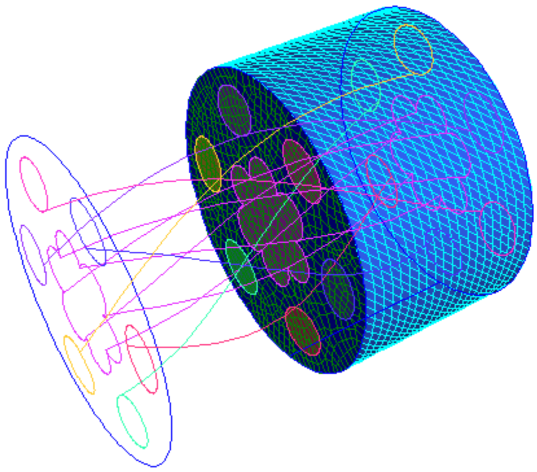

Figure 0.10 Face are un-hidden and used for reference for further extrusion of model

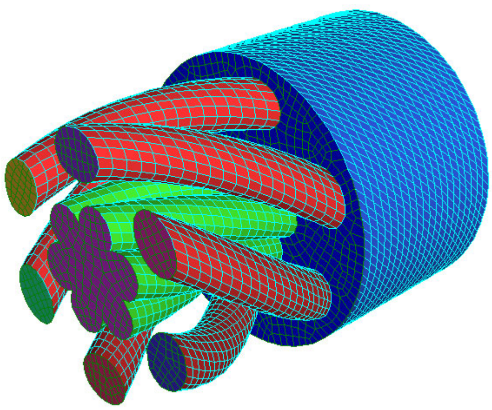

Figure 0.11 By using the custom UCS ferrule connector and SWR can be further extruded.

By creating this section of assembly, it is possible to copy and paste the same section to create a multiply ferrule assembly.

This is done by going to **Tool-Copy-By Increments** and repeating the increments by 2 times.

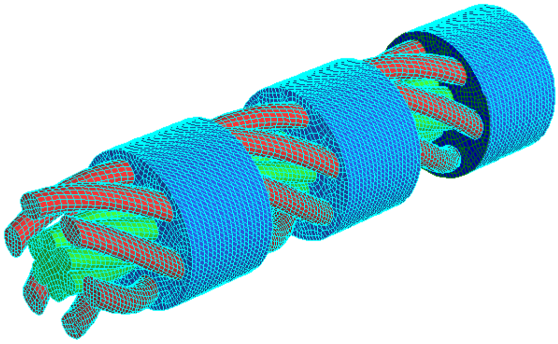

This leaves the assembly with extra length of steel wire rope and ferrule connector wire. This is manually deleted and leave us with a 3-ferrule connector assembly. If further ferrules are required, copy by increment function in Strand 7 can be repeated to make 5, 7, 9 ore more ferrules assemblies.

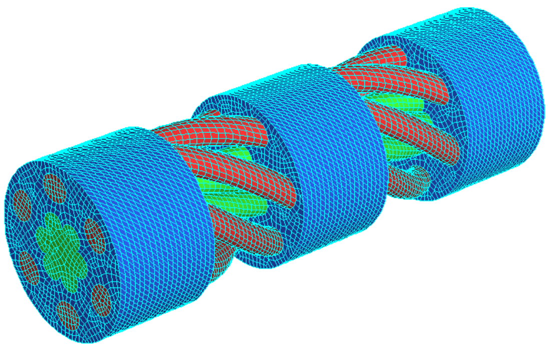

Figure 0.12

Step 6 – Solving Assembly

With the assembly complete, contact must be place between ferrule connectors and ferrule

This is can be done by going to **Attributes – Attachments**, from there creating a **flexible** beam element.

A maximum gap distance is required to ensure that contacts elements do not connector with other parts of the assembly.

From here, use **the Tools – Attach Parts** function, refine source and target details then click apply.

This will produce a contact as shown below.

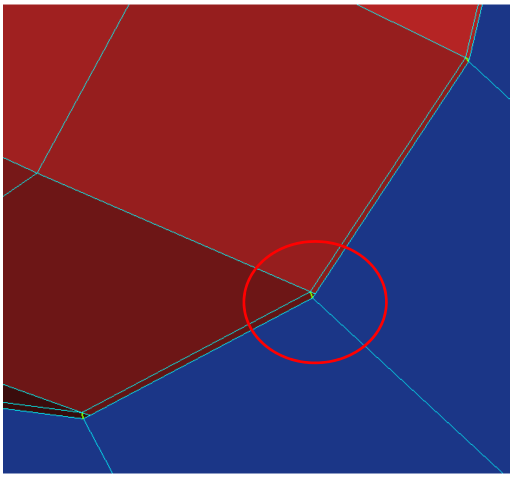

Figure 0.13

Each component in the assembly is allocated its own properties i.e. modulus, material type stiffness etc. and can be done through the **Properties** tab

Once each component has defined properties. Loads and restraints can then be applied.

The model below shows that assembly is restrained at one end of the wire, the other end has an axial load applied.

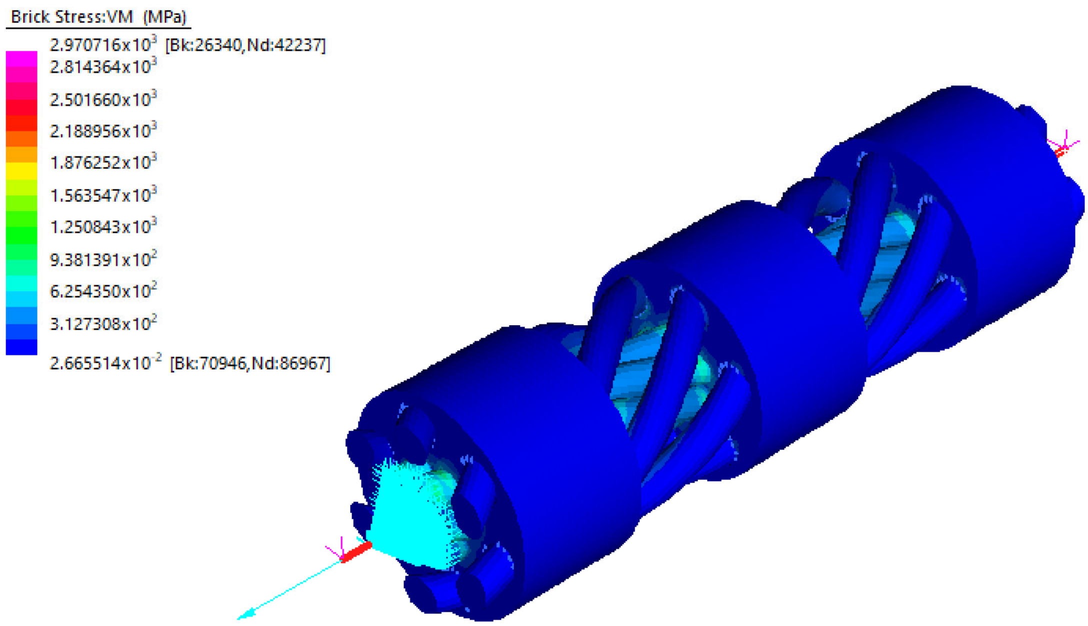

The model is solved using a Nonlinear Static Analysis loaded over four increments. If not solved in step/increments it can be difficult to converge on solution.